OPTICAL CONTROL OF NUCLEAR RESONANT ABSORPTION: THEORY AND EXPERIMENT

A Dissertation

by

ROMAN L. KOLESOV

Submitted to the Office of Graduate Studies of
Texas A&M University
in partial fulfillment of the requirements for the degree of

DOCTOR OF PHILOSOPHY

May 2004

Major Subject: Physics

OPTICAL CONTROL OF NUCLEAR RESONANT ABSORPTION: THEORY AND EXPERIMENT

A Dissertation

by

ROMAN L. KOLESOV

Submitted to Texas A&M University
in partial fulfillment of the requirements
for the degree of

DOCTOR OF PHILOSOPHY

Approved as to style and content by:

Olga Kocharovskaya (Chair of Committee)	
George R. Welch (Member)	Edward S. Fry (Member)
Timothy R. Hughbanks (Member)	Edward S. Fry (Head of Department)

May 2004

Major Subject: Physics

ABSTRACT

Optical Control of Nuclear Resonant Absorption:
Theory and Experiment. (May 2004)
Roman L. Kolesov, B.S., Nizhny Novgorod State University, Russia;
M.S., Nizhny Novgorod State University, Russia
Chair of Advisory Committee: Dr. Olga Kocharovskaya

Modification of nuclear resonant absorption by means of laser radiation is analyzed both theoretically and experimentally. Theoretical analysis is done on the basis of four-level model of atom. This model includes both electronic and nuclear excitations. It is predicted that under coherent laser driving nuclear resonant Mössbauer absorption can be significantly modified, e.g. new Mössbauer resonances can appear, some of the existing resonances can vanish, both can be Rabi-split, broadened by laser action. In addition, it is predicted that Mössbauer absorption can be completely suppressed due to coherent population trapping. Experimental observation of laser-induced transformations of Mössbauer spectra of $^{57}Fe^{2+} : MgO$ is accomplished. New Mössbauer lines appear with laser driving while the existing are broadened. Possible explanations of the observed changes in $^{57}Fe^{2+} : MgO$ Mössbauer spectra are population of higher-lying electronic states of iron ion and significant modification of electronic relaxation processes due to modified Jahn-Teller interaction.

ACKNOWLEDGMENTS

I would like to thank my research advisor Prof. Olga Kocharovskaya and my co-workers Farit Vagizov, Elena Kuznetsova, Serguei Lissotchenko, Yuri Rostovtsev, and Nikolai Kalugin for fruitful joint work, valuable discussions, and continuous help in conducting my research. It was my real pleasure to work with these people.

TABLE OF CONTENTS

CHAPTER Page

LIST OF FIGURES

FIGURE Page

FIGURE Page

FIGURE Page

CHAPTER I

INTRODUCTION

In recent years very much attention has been paid to studying interference optical effects caused by coherent interaction of laser radiation with multi-level (mostly, three- and four-level) media. It turns out that atomic coherence leads to many interesting and unexpected phenomena such as lasing without population inversion [1] (LWI), electromagnetically induced transparency [2] (EIT), and enhanced index of refraction without absorption [3]. Typically, optical interference effects occur in multi-level media (more than two levels) under additional coherent driving by strong coupling laser field. Proof-of-principle experimental demonstrations of inversionless gain [4], large index of refraction without absorption [5], and the first lasers without inversion [6] have stimulated further investigations in this field. The researchers' interest in studying atomic interference phenomena can be explained by wide range of potential applications of the effects mentioned above. Let us consider some of them.

We start with LWI. It is well known that in order to obtain laser action at higher frequencies (ultraviolet, x-rays, γ-rays) one should overcome many difficulties. One of them is that with increasing the frequency ω of operating atomic laser transition the pump power required to produce population inversion (if it is ever possible) scales as ω^3 according to radiative spontaneous decay time drop. Consequently, it becomes harder and harder to produce population inversion as the desired laser wavelength decreases. However, LWI offers one a possibility to make the condition of population inversion at operating transition unnecessary for laser generation. Thus, LWI would significantly reduce requirements for pumping intensity.

The journal model is Physical Review A.

Another interesting optical interference phenomenon - EIT - attracts much attention because of extensive works on the problem of quantum computer. As it was demonstrated recently, EIT-related effects can be used for quantum information storage [7]. EIT is accompanied by another interesting phenomenon - reduction of the group velocity of light [8]. The term "slow light" is already widely known. This effect can be used in optical delay lines in communication networks.

Implementations of EIT- and CPT-related effects are not restricted by possible applications in quantum computers. Rather recently, a technique for producing ultrashort optical pulses based on atomic-coherence-related effects was proposed in works [9]. It was successfully demonstrated, both theoretically and experimentally, that by use of atomic coherence one can generate wide coherent optical spectra and compress the output multi-colored signal into a sequence of ultrashort pulses. However, the repetition rate of the generated pulse sequence is very high (tens of THz). To lower the repetition rate, it was proposed to use Zeeman or hyperfine coherence in solids for broadband optical generation [10]. If realized experimentally, the improved technique of ultrashort pulse generation, proposed by us, would allow one to obtain pulse durations $\sim 1\ fs$ at GHz repetition rates.

Another possible application of EIT/CPT-related effects would be sensitive magnetic diagnostics of plasmas. Currently, existing methods of measuring magnetic field inside plasma either invasive, i.e. disturbing plasma parameters, or non-local. In [11] we proposed to detect both the magnitude and the direction of the magnetic field by measuring CPT resonances in laser-induced fluorescence. Proof-of-principle experiments were done in neon glow discharge. This method of magnetic field measurements is local, non-invasive, and highly-sensitive (compared to existing plasma diagnostics). It is worth to note, that previously non-linear Faraday rotation, accompanying EIT, was already proposed for high-resolution magnetometry [12].

Effects, similar to EIT and LWI, could be seen in the gamma-ray range if it were possible to observe resonant nuclear absorption and to drive nuclear transitions coherently. The first requirement is fulfilled due to existence of the Mössbauer effect [13].

Mössbauer effect manifests itself in recoilless and unbroadened γ-ray emission and absorption at nuclear transitions if corresponding nuclei are embedded in a solid host. For a free atom nuclear emission and absorption bands are broadened due to Doppler effect. In addition, they are shifted with respect to each other by the value twice the recoil energy of γ-ray photon emission/absorption. This energy is equal to $E_{rec} = \hbar^2\omega^2/2Mc^2$, where ω is the γ-ray photon frequency and M is the mass of an atom. It is easy to explain, because for the photon to be absorbed by a nucleus its energy should be enough to excite nuclear transition and, simultaneously, make the atom move. Thus, nuclear absorption is blue-shifted with respect to nuclear transition energy. Vice versa, the emitted γ-ray photon is red-shifted with respect to nuclear excitation energy.

Doppler broadening of nuclear emission and absorption transitions is caused by thermal motion of emitting/absorbing atoms. The value of this broadening is $v_T\omega/c$, where v_T is the thermal velocity of atoms. Below, estimates for recoil energy and Doppler broadening of nuclear γ-ray transitions will be given.

The natural linewidths of nuclear transitions can vary in a very broad range: from a few attoseconds (light elements, high-energy transitions) to several years (one of the examples is an isomer state of ^{178}Hf which lives $\sim 31\ years$). However, for not very high nuclear excitations up to $\sim 100\ keV$ radiative lifetimes are typically in the microsecond through picosecond range. For example, for a well-known 14.4 keV excitation in ^{57}Fe the lifetime is 100 ns. This means that the Q-factor of a typical nuclear transition is very high. For the above example of ^{57}Fe it is 2×10^{11}. Thus, it

would be very attractive to use nuclear transitions for sensitive spectroscopy. However, for free atoms thermal Doppler broadening is huge. For example, for the same $14.4keV$ transition of ^{57}Fe it can be estimated as $\sim 10^4$ natural linewidths at room temperature. Moreover, Doppler width behaves as $\sqrt{T}$, where T is the temperature. Thus, to make the width of nuclear absorption or emission resonance comparable to the natural one, it is necessary to cool atoms down to microkelvin temperatures.

The estimates for the energy difference for nuclear emission and absorption for the above example give the value $\sim 10^5$ natural linewidths. Thus, the emission and absorption spectra of ^{57}Fe nucleus do not overlap.

However, the situation changes drastically if the emitting/absorbing nucleus is embedded into a solid host. In this case there is a finite probability for the nucleus to emit or absorb γ-ray photon almost without recoil. The word "almost" means that the recoil momentum is transferred to the host rather than to a single atom. The recoil energy for this process is decreased by the ratio $M/M_{crystal}$, where M is, again, the mass of one atom and $M_{crystal}$ is the macroscopic mass of the host. It is easy to see, that this ratio is extremely small ($10^{-15} \div 10^{-20}$). Thus, the energy difference between nuclear emission and absorption energies becomes negligible. Moreover, recoilless emission/absorption eliminates thermal Doppler broadening because γ-ray photon energy is affected by the motion of the whole macroscopic sample rather than by the motion of a single atom. As a result, the spectral width of the emission and absorption nuclear resonances becomes close to the natural one. Thus, it becomes possible to observe extremely narrow nuclear resonances experimentally.

A powerful spectroscopic technique on the basis of the described phenomenon of nuclear recoilless emission and absorption exists. It is called Mössbauer spectroscopy [14]. It is widely used in nuclear and solid-state physics, in geology, biology, chemistry, material science, etc. In order to make any kind of spectroscopy, one has to have an

emitter and an absorber. In Mössbauer spectroscopy recoilless γ-decay of excited nuclear transitions serves as a source of narrow-band γ-radiation. At the same time, ground-state nuclei of the same type serve as an absorber. By measuring the change in the number of γ-ray photons penetrating through the absorber as a function of relative velocity of the absorber and the source, one can study the nuclear absorption spectra of different solids. Since the linewidth of Mössbauer transition is very narrow, one can study parameters of hyperfine interactions of the absorbing nucleus with its surrounding. In turn, from these parameters one can deduce many characteristics of solids, such as local strains, magnetic fields, electrical field gradients, electron density at the nucleus, etc.

Due to extremely high Q-factor of nuclear transitions, they are very sensitive to any changes in nuclear environment. Thus, it is easy to affect resonant nuclear spectra by external radiation in incoherent or coherent manner. This can be done by affecting nuclear transitions directly or through surrounding electrons. On this basis, a new spectroscopic technique was proposed recently in [15]. It deals with modification of the Mössbauer spectra under the action of an optical laser radiation. These modifications can be manifested as one or more of the following: suppression of gamma-ray absorption, appearance of additional or vanishing of the existing lines in the Mossbauer spectrum, changes in the line widths and line positions, and additional splitting of the lines. Experimental realization of coherent effects in γ-ray optics would help much in resolving a long-standing problem of γ-ray laser [16]. Unfortunately, up to now these theoretical predictions are not verified experimentally.

In the present work a possibility of laser modification, manipulation, and control of nuclear resonant absorption is considered both theoretically and experimentally. Dissertation is organized in the following way.

In Chapter II different ways of coherent driving of nuclear resonant transitions are

reviewed. There will be discussed vibrational modulation of Mössbauer spectra, radio-frequency driving of nuclear hyperfine transitions, and incoherent optical pumping of long-lived molecular configurational states in sodium nitroprusside and related compounds.

In Chapter III a possibility to drive nuclei coherently by means of laser radiation will be considered theoretically. The chapter starts with review of types of hyperfine interactions. After that, a simplified model of Mössbauer absorber as a four-level medium interacting simultaneously with laser driving and γ-ray probe fields will be introduced. It will be shown that in the absence of hyperfine interaction between the nucleus and its electronic surrounding there is no effect of laser field on nuclear resonant absorption. However, if there is a hyperfine interaction between the nucleus and the electronic shell of a corresponding ion, one would expect very strong modifications of Mössbauer spectra. Two cases are considered: 1) isomer shift of atomic levels in the four-level system and 2) hyperfine splitting of the ground state. Possible transformations of Mössbauer spectra are predicted for both.

Finally, in Chapter IV a laser-Mössbauer experiment done with $^{57}Fe^{2+} : MgO$ crystal is described. The section starts with general consideration of the requirements for Mössbauer absorber that should be fulfilled to do laser-Mössbauer experiments. Not all elements possess Mössbauer transitions. The reason for that is that for very high nuclear excitations the rigidity of the solid host is not sufficient to make the probability of recoilless emission and absorption high enough. Thus, only those nuclei, which have transitions within the range $5 \div 100\ keV$ can be Mössbauer-active. The solid host should be transparent for optical radiation. In addition to that, Mössbauer-active ions incorporated into a transparent host should exhibit narrow electronic resonances in the optical range in order to be efficiently driven by laser radiation. Classes of materials suitable for experimental purposes are identified. These are transition-

metal doped and rare-earth doped optical crystals. The two Mössbauer elements are of particular interest: iron-57 and europium-151. Several candidate crystals doped with these elements are chosen. Estimates of laser intensity required to observe light-induced changes in Mössbauer spectra are presented. Among them the crystal of MgO doped with $^{57}Fe^{2+}$ was chosen for the laser-Mössbauer experiment. The sample preparation procedure and the experimental setup are described. Significant changes in the Mössbauer spectrum of the sample under study are observed under laser action. Even though no satisfactory explanation of the observed laser-induced changes is found so far, several possible versions are presented. Among them is laser excitation of metastable electronic or configurational states of $^{57}Fe^{2+} : MgO$.

CHAPTER II

OVERVIEW OF MODIFICATIONS OF MÖSSBAUER SPECTRA BY MEANS OF EXTERNAL DRIVING

In this chapter an overview of possible modifications of Mössbauer absorption spectra by means of external coherent driving is given. As was discussed in the Introduction, Mössbauer transitions are extremely sensitive to the nuclear surrounding. Thus, nuclear resonant absorption spectra can be rather easily altered by changing electronic and/or vibrational states of the crystal, its temperature, by applying magnetic field, etc.

A. Vibrational Modulation of Mössbauer Spectra

We start with periodic modulation of Mössbauer γ-ray quanta by mechanical motion of either Mössbauer source or absorber. In fact, Mössbauer spectroscopy itself relies on a possibility to change the energy of the emitted γ-ray quanta by changing the velocity of the emitting nucleus. However, the time-scale of the velocity change in a typical Mössbauer setup is much longer than the nuclear lifetime. Indeed, if the time-scale of the motion is comparable or even shorter than the inverse nuclear linewidth, many interesting effects can be observed.

One of the first experimental works in this area was done by Heiman et al. in 1968 [17]. In this work a number of additional acoustic sidebands in the Mössbauer absorption spectrum of metallic iron was observed. An ultrasound wave was generated via magnetostriction due to applied radio-frequency ($\approx$ 13 MHz) magnetic field. Magnetostriction manifests itself as contraction of the crystal sample placed in a sufficiently strong magnetic field. Periodical modulation of the magnetic field excites sound waves of corresponding frequency (twice the frequency of modulation, because

the crystal contraction does not depend on the magnetic field direction) in the crystal. In turn, the acoustic wave produces Doppler shift of the nuclear transition energy. Finally, periodically modulated Doppler shift causes the appearance of acoustically excited sidebands in the absorption spectrum.

The work cited above and the related one [18] have started a new branch of research in the Mössbauer spectroscopy, namely, study of transient effects in the nuclear resonant absorption. Later, coherent transient effects due to phase modulation of γ-rays were extensively studied by finish group of Katila [19]. In their works a narrow-linewidth Mössbauer isotope ^{67}Zn was used. In these works counting rate of γ-quanta emitted by a vibrating source and passing through a resonant absorber was studied as a function of the vibration phase. It was shown both theoretically and experimentally that counting rate is modulated due to interference of the incident γ-quanta and the polarization excited by them in the Mössbauer absorber. In one of our recent works we proposed an extension of the work done by finish group [20]. Namely, if one uses far detuned resonant Mössbauer absorber, it is possible to compress vibrationally modulated γ-rays into a train of short pulses. The duration of these pulses can be made much smaller than the lifetime of the excited state of the Mössbauer transition.

One more branch of transient Mössbauer studies deals with so called gamma-echo [21]. It is known that resonant γ-quanta passing through an optically thick Mössbauer absorber decay much faster than the lifetime of the excited Mössbauer state due to saturation of absorption [22]. However, if the absorber is suddenly moved by half-wavelendth within the lifetime of the source excited nucleus after its formation, gamma-radiation can be regenerated. This happens due to interference of the source radiation and nuclear polarization excited in the absorber by the same radiation and phase-shifted by π. Experiments in this field have been done rather

extensively in a various configurations and with both conventional and synchrotron Mössbauer sources [23].

B. Radio-Frequency Driving and Rabi-Splitting of Mössbauer Lines

Another possible way to affect resonant nuclear transitions is a direct driving of nuclear hyperfine transitions with external radio-frequency (RF) or microwave electromagnetic field. In this case it is possible to observe Rabi-splitting of Mössbauer lines by the value of driving field Raby-frequency. This was successfully demonstrated by Vagiziov [24]. However, such an experiment requires lots of experimental efforts. First of all, Rabi frequency of the applied RF field should exceed nuclear linewidth. Thus, very high RF power is required. Consequently, special precautions should be taken in order not to burn the Mössbauer absorber. Lastly, as we have seen in the previous section, strong magnetic fields of varing amplitude would lead to magnetostriction and, thus, to appearance of vibrational Mössbauer satellites. However, if circularly polarized RF field is applied, the absolute value of the magnetic field will always be the same. This would allow one to get rid of magnetostriction effects.

C. Mössbauer Spectra of Optically-Pumped Metastable States in Sodium Nitroprusside and Related Compounds

As was already mentioned above, the shape of Mössbauer spectrum strongly depends on nuclear electronic surrounding. Thus, if crystal is subject to some photochemical reactions, nuclear surrounding can be altered by either coherent (laser) or incoherent light. This was demonstrated in 1977 by Hauser et al. in the Mössbauer study of optically illuminated sodium nitroprusside [25].

In these experiments samples of sodium nitroprusside $(Na_2 [Fe (CN)_5 NO] \cdot$

$2H_2O$) were illuminated with blue-green light (typically, argon laser with a wavelength either 514.5 nm or 488 nm) and the Mössbauer absorption spectrum was collected after illumination. It came out, that there is some optically induced metastable state whose lifetime at temperatures below 160 K is almost infinite ($T \gg 10^7$ s at 100 K). Its Mössbauer spectrum has larger quadrupole splitting and different isomer shift than the ground state. In the works cited above it was shown that almost 45% of all molecules can be excited into this metastable state. It was also pointed out that population of metastable state occurs only for certain polarization of incident light.

Later on, the second optically excited metastable state of sodium nitroprusside was discovered. It can be excited from the first metastable state by illuminating the sample with infrared or red light. Moreover, other iron-containing compounds were discovered to possess similar properties [26].

Despite the fact that long time passed since the discovery of optically excited metastable states in sodium nitroprusside and related compounds, no final conclusion is made so far about the origin of these states. It is, however, established that the excitation of these states has to do with optical reorientation of $N-O$ bond in nitrosyl anion (see, for example, [27]).

However, the effect of populating metastable electronic state on Mössbauer absorption is rather obvious, even though it gives much spectroscopic information about the sample under study. It would be interesting to study the dynamic effects of coherent/incoherent optical radiation on nuclear resonant absorption. Theoretical consideration of this problem would require suitable model which would include dynamics of both nuclear and electronic subsystems. This is done in the next chapter.

CHAPTER III

INTERACTION OF COMBINED ELECTRON-NUCLEAR SYSTEM WITH RADIATION

In order do describe quantitatively how nuclear resonant spectra can be affected by optical radiation, a model of how electronic excitation is transferred to the nucleus should be developed. This transfer can be accomplished by hyperfine coupling of electronic and nuclear subsystems. Even though this coupling is very weak (typical values of hyperfine interactions are in $MHz - GHz$ frequency range), it can substantially affect nuclear resonant spectrum since typical linewidths of Mössbauer transitions are even lower. Let us consider different types of hyperfine interactions.

A. Hyperfine Interactions

Hyperfine interactions arise from two facts: 1) charge is distributed inside the nucleus and 2) most nuclei have non-zero magnetic moment. Consequently, spherically symmetric or non-symmetric nuclear charge distribution leads to different types of electrostatic interaction with electric field produced by electrons while non-zero nuclear magnetic moment can interact with magnetic field at nuclear site.

1. Isomer Shift

This type of hyperfine interaction is the most common one. The physical origin of isomer shift is finite radius of the nucleus. It can be described by using a very simple model of a hydrogen-like atom possessing one s-electron (see Fig.1). If nuclear radius was zero, its electrostatic potential would have been a simple $1/r$ Coulomb potential, where r is the distance from the center of nucleus (curve $1/r$ on Fig.1). However, in reality nuclear radius is finite. This leads to the removal of singularity

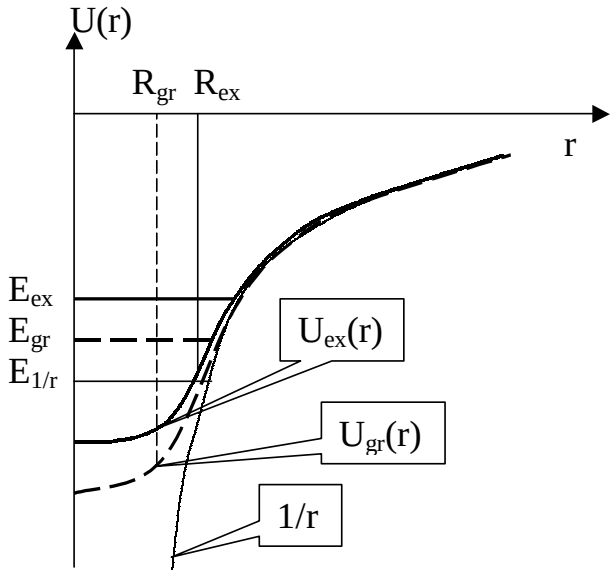

Fig. 1. Shift of s-electron energy as nuclear radius is changed. Here $U_{gr}(r)$ and $U_{ex}(r)$ are the electrostatic potentials for the ground-state and for the excited-state nucleus, R_{gr} and R_{ex} are corresponding nuclear radii, $E_{1/r}$, E_{gr}, and E_{ex} represent electron energies for the potentials $1/r$, $U_{gr}(r)$, and $U_{ex}(r)$ respectively.

in nuclear potential at the origin (curve $U_{gr}(r)$ on Fig.1). Thus, the energy of the electron moving in the electrostatic potential of the nucleus is shifted up with respect to the case of zero nuclear radius. The value of this shift depends on both nuclear radius and the electronic density at nuclear site. Mostly, s-electrons are affected by the electrostatic interaction with nuclear charge distribution because only s-electrons have non-zero density at nuclear site. In turn, if the radius is changed due to nuclear excitation, the form of the nuclear electrostatic potential is also changed. This would lead to energy shift of the electronic state. This shift is called isomer shift.

Isomer shift of Mössbauer transition is a very important quantity in the Mössbauer spectroscopy. The shift of nuclear transition energies can be observed for different chemical compositions of the absorber. In this case it is called chemical isomer shift. It contains lots of information about nucleus itself, about variation of electronic charge

density at the nucleus as the chemical composition is altered, about absorber temperature, etc. The value of chemical isomer shift is given by the formula:

$$\delta_{Isomer} = \frac{4\pi}{5} e^2 Z R^2 \frac{\Delta R}{R} \left[|\Psi(0)|_a^2 - |\Psi(0)|_s^2 \right]. \tag{3.1}$$

Here Z is the nuclear charge, R is its radius, ΔR is the change of radius due to nuclear excitation, and $|\Psi(0)|_{s,a}^2$ are the electron densities at nuclear site for the source and absorber respectively. In the conventional Mössbauer spectroscopy the change in electron density at the nucleus is caused by different chemical environment. However, it can be altered by other ways, for example, by exciting electronic shell of the ion.

It is worth to note, that isomer shift is closely related to isotope shift of electronic transitions for different isotopes of the same element. In both cases the difference in energies of electronic states originates from different nuclear radii. In the case of isotope shift the difference in radii comes from different number of neutrons inside the nucleus while in the case of isomer shift nuclear excitation is responsible for the change. It is also worth to say, that isomer shift of electronic transitions was already successfully observed in some gaseous media [28].

2. Quadrupole Interaction

Quadrupole hyperfine interaction is a different kind of electrostatic interaction of the nucleus with its surrounding. It occurs if nuclear charge distribution is not spherically symmetric. In this case nucleus possesses quadrupole electric moment. If, in turn, crystal field at the nucleus has rather low symmetry, it produces electric field gradient. The interaction of nuclear quadrupole moment with gradient of the electric crystal field can be described by a classical Hamiltonian:

$$H_Q^{(class)} = \sum_{ij} Q_{ij} \frac{\partial E_i}{\partial x_j}, \tag{3.2}$$

where Q_{ij} denotes nuclear quadrupole tensor, E_i is the i-th component of the electric field, and x_j is the j-th Cartesian coordinate. Nucleus is situated in the local minimum of the electrostatic potential of the crystal $V(x_j)$. Thus, $\partial V/\partial x_j = 0$ since nucleus is at the equilibrium position. However, the second spatial derivatives are non-zero in general ($\partial^2 V/\partial x_i \partial x_j \neq 0$). These derivatives form electric field gradient tensor. By appropriate choice of coordinates, this tensor can be written in the diagonal form with V_{xx}, V_{yy}, and V_{zz} being the only non-zero components (all three positive). Conventionally, the largest value is chosen to be V_{zz}. Quantum Hamiltonian for nuclear quadrupole interaction can be written in the following form:

$$H_Q^{(quant)} = Q\left(3I_z^2 - I(I+1) + \frac{\eta}{2}\left(I_+^2 + I_-^2\right)\right). \tag{3.3}$$

Here Q represents the strength of quadrupole interaction including the value of nuclear quadrupole moment and the value of electric field gradient, I is nuclear spin, I_z is the spin projection onto the quantization axis, $I_\pm$ are usual raising and lowering spin operators, and η is asymmetry parameter. The asymmetry parameter represents possible difference of V_{xx} and V_{yy}. It is equal to unity for axially-symmetric crystal field and less than unity otherwise.

Equation (3.3) clearly shows that quadrupole interaction can occur only for nuclear states with $I \geq 1$. Furthermore, high symmetry of the crystal field removes quadrupole interaction. This happens, for example, in cubic and octahedral sites. This situation was observed in the Mössbauer spectrum of $^{57}Fe^{2+}$-doped III-V semiconductors [29]. However, cubic symmetry can be lowered by lattice vibrations (Jahn-Teller effect). In this case quadrupole splitting can occur even in octahedral or cubic sites of Mössbauer ions.

3. Magnetic Hyperfine Interaction

The third type of hyperfine interactions arises due to coupling of nuclear magnetic moment to the magnetic field present in the crystal at nuclear site. The origin of the magnetic field is not essential for appearance of magnetic hyperfine structure. It can be external, can originate from magnetic properties of the material (ferromagnetism or anti-ferromagnetism), or it can be of paramagnetic origin. In all three cases the interaction Hamiltonian can be written in the form:

$$H_M = \mu_n \mathbf{B} \cdot \mathbf{I}, \tag{3.4}$$

where $\mathbf{B}$ is the magnetic field vector, $\mathbf{I}$ is nuclear spin, and μ_n is the value of nuclear magnetic moment.

Magnetic hyperfine interaction occurs only for nuclei with non-zero spin. Typically, observation of magnetic hyperfine structure by means of Mössbauer spectroscopy allows one to obtain information about the anti-/ferromagnetic field inside the crystal, its direction, temperature dependence for studying magnetic phase transitions, parameters of electron exchange interaction, etc.

B. Simplified Four-Level Model of an Atom

In order to describe quantitatively which parameters of nuclear hyperfine interactions can be affected by optical radiation being in resonance with some electronic transition, the following simplified model of the combined electron-nuclear system can be developed [15]. Both electronic and nuclear degrees of freedom can be viewed as two level systems. Of course, in reality the situation is more complicated, since both electronic and nuclear subsystems have very many energy states. The combined structure of energy levels is shown in Fig.2. The lowest energy state 1 corresponds to the ground

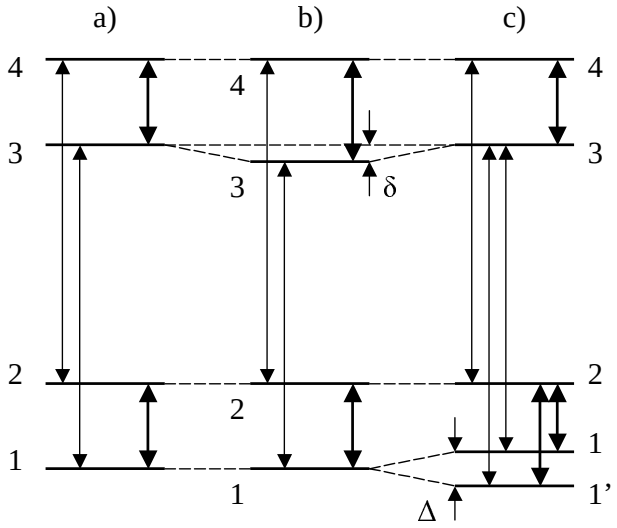

Fig. 2. Simplified 4-level scheme of the combined nuclear-electronic system. Three cases are indicated: a) no hyperfine coupling, b) isomer shift of levels, and c) hyperfine splitting of the ground-state level. Bold two-headed arrows show optical electronic transitions while thin two-headed arrows indicate γ-ray nuclear transitions.

state of both electronic shell and nucleus. The first excited state 2 corresponds to optical excitation of the electronic shell while nucleus still stays in the ground state. Vice versa, the second excited level 3 represents the atom with ground-state electronic subsystem and excited nucleus. Finally, the third excited state 4 corresponds to excitation of both nucleus and electronic shell. Consequently, there are two electronic optical transitions, $1 \leftrightarrow 2$ and $3 \leftrightarrow 4$, corresponding to the ground- and excited-state nucleus respectively. Vice versa, there are two nuclear γ-ray transitions, $1 \leftrightarrow 3$ and $2 \leftrightarrow 4$, corresponding to the ground and excited states of the electronic shell. We assume that combined transitions, in which states of both electronic shell and nucleus are changed, are forbidden.

If there is no coupling between electronic and nuclear degrees of freedom, nuclear transitions in both ground and excited electronic states have the same characteristics

(see Fig.2a). Same holds true for electronic transitions for the ground and excited states of the nucleus. However, if one includes hyperfine coupling into consideration, the situation changes. Let us consider first the simplest case of different Mössbauer isomer shifts for the ground and excited states of the electronic shell. In this case the frequency differences $\omega_{31} - \omega_{42} = \omega_{21} - \omega_{43}$ are equal to the isomer shift value δ (see Fig.2b). Furthermore, one or more states of the combined system can be split by either electric quadrupole and/or magnetic interactions (see Fig.2c). In general, these splittings are different for all four energy levels. The symmetry of the initial four level system is now removed by hyperfine interactions.

In the next section we will discuss which differences in the Mössbauer absorption spectra can be observed under the action of control optical field if hyperfine parameters of the four energy states of the combined electron-nuclear system are distinct.

C. Possible Modifications of Nuclear Resonant Absorption due to Optical Driving for Different Hyperfine Interactions

Let us consider theoretically possible changes in the Mössbauer absorption spectra by means of either coherent or incoherent optical driving. The analysis will be done on the basis of semi-classical density matrix approach when both optical driving and γ-ray probe fields are considered classically while ions are considered as a combination of two quantum subsystems: electronic and nuclear.

1. Isomer Shift

We start with the simplest case of isomer shift of atomic levels with no other hyperfine interactions present. In order to describe the interaction of the 4-level medium with radiation (both γ-rays and control laser field, resonant with electronic transition),

the following assumptions are used. First, of all we consider both optical and γ-ray fields to be classical ones. This approximation is certainly valid for the strong optical field, but its validity is questionable for γ-rays since in most Mössbauer experiments only one γ-quantum can be present in the medium instantaneously. In other words, γ-quanta are counted one by one, so that each time the medium interacts with only one γ-quantum. However, the approach, in which γ-radiation is treated classically, works rather well in explaining most Mössbauer data.

Secondly, both γ-rays and optical radiation are considered being monochromatic plain waves propagating along z-direction:

$$E_{opt,\gamma} = \frac{1}{2}\left(E_{d,p}e^{-i\omega_{d,p}t+ik_{d,p}z} + c.c.\right). \tag{3.5}$$

Here $E_{opt,\gamma}$ are the electric fields of driving optical and probe gamma fields, $E_{d,p}$ are corresponding slow varying envelopes, and $\omega_{d,p}$ and $k_{d,p}$ are corresponding frequencies and wavenumbers.

As for the medium (combined electron-nuclear system), the following assumptions are used:

- Electronic transitions in both ground and excited states of the nucleus have the same parameters (transition dipole moments, population relaxation rates, etc.) except for the frequency. The frequencies differ by the value of isomer shift δ. Same is true for the nuclear transitions in the ground and excited states of the electronic shell.

- Nuclear transitions are assumed to be of natural linewidth, i.e. the width of Mössbaue transitions is determined by nuclear lifetime. However, electronic transitions can be broadened both homogeneously and inhomogeneously. This situation is rather typical in solids. In good-quality crystals Mössbauer tran-

sitions of rather short-lived nuclear isotopes are not significantly broadened, while even a very good crystals optical transitions are several orders of magnitude broader than their natural linewidth.

- All relaxation processes lower the energy of the electron-nuclear system. This means that the temperature of the medium is lower than the energy of electronic transitions. As a result, at electronic transitions population can decay via transitions $2 \to 1$ and $4 \to 3$, but not via $1 \to 2$ and $3 \to 4$. Thus, in the absence of both driving and probe fields only state 1 is populated.

- It is assumed that there is no feedback effect of the medium on the driving field. This assumption is valid if driving laser field is strong enough.

Let us right down the equations governing absorption of probe field at transitions $1 \to 3$ and $2 \to 4$. In doing this we assume that probe field does not affect the state of the system in a sense that no population redistribution and no affect on coherences at optical transitions is caused by the probe field. This allows one to use a perturbation theory to treat the problem quantitatively. The zeroth order equations of motion for the density matrix elements describe populations of the two lower states of the medium and the optical coherence at the transition $1 \leftrightarrow 2$:

$$\frac{d\rho_{11}}{dt} + i\left(\Omega_d \sigma_{12} - \Omega_d^* \sigma_{21}\right) = w_{21}\rho_{22}, \tag{3.6}$$

$$\frac{d\sigma_{21}}{dt} + i\left(\omega_{21} - \omega_d\right)\sigma_{21} + i\Omega_d\left(\rho_{22} - \rho_{11}\right) = -\gamma_{21}\sigma_{21}, \tag{3.7}$$

$$\rho_{11} + \rho_{22} = 1. \tag{3.8}$$

Here the followng notations are introduced: 1) ρ_{mm} is the population of m-th level; 2) σ_{mn} is the coherence amplitude at the transition $m \leftrightarrow n$ averaged over ω_p for γ-ray transitions and over ω_d for optical transitions; in the particular case (3.7) σ_{21} is the

complex amplitude of the coherence at $1 \leftrightarrow 2$ transition, $\rho_{21} = \sigma_{21} \exp(-i\omega_d t + ik_d z)$; 3) w_{21} is the population decay rate at optical transition $2 \rightarrow 1$; 4) γ_{21} is the decoherence rate at optical transition $1 \leftrightarrow 2$, $\gamma_{21} = w_{21}/2 + \gamma_{deph}$, where γ_{deph} represents decoherence processes not related to population decay; 5) $\Omega_{d,p}$ represents Rabi frequency of the corresponding field, driving or probe, $\Omega_{d,p} = E_{d,p}\mu_{d,p}/2\hbar$, $\mu_{d,p}$ is the corresponding transition dipole moment. All other coherences and populations are equal to zero in the zeroth order approximation.

The first order approximation takes into account excitation of coherences at nuclear transitions due to interaction of the medium with the probe field. In this approximation populations of the upper states 3 and 4 are still zeroes, so that the optical coherence $\sigma_{43} = 0$. However, σ_{31}, σ_{42}, σ_{41}, and σ_{32} become non-zero since they are proportional to the first order of the probe field amplitude. At the same time, ρ_{33}, ρ_{44}, and σ_{43} are proportional to the probe field intensity (square of the amplitude) and can be neglected. The set of first order equations can be written in the following way:

$$\frac{d\sigma_{31}}{dt} + i(\omega_{31} - \omega_p)\sigma_{31} + i\Omega_p(\rho_{33} - \rho_{11}) - i\Omega_d^*\sigma_{41} + i\Omega_d\sigma_{32} = -\gamma_{31}\sigma_{31} + \gamma_{cross}\sigma_{42}, \quad (3.9)$$

$$\frac{d\sigma_{42}}{dt} + i(\omega_{42} - \omega_p)\sigma_{42} + i\Omega_p(\rho_{44} - \rho_{22}) + i\Omega_d^*\sigma_{41} - i\Omega_d\sigma_{32} = -\gamma_{42}\sigma_{42}, \quad (3.10)$$

$$\frac{d\sigma_{41}}{dt} + i(\omega_{41} - \omega_d - \omega_p)\sigma_{41} - i(\Omega_d\sigma_{31} + \Omega_p\sigma_{21} - \Omega_d\sigma_{42}) = -\gamma_{41}\sigma_{41}, \quad (3.11)$$

$$\frac{d\sigma_{32}}{dt} + i(\omega_{32} - \omega_p + \omega_d)\sigma_{32} - i(\Omega_p\sigma_{12} + \Omega_d^*\sigma_{42} - \Omega_d^*\sigma_{31}) = -\gamma_{32}\sigma_{32}. \quad (3.12)$$

All the notations have already been introduced previously except for γ_{cross} which is the cross-relaxation rate at nuclear transitions. It occurs due to the fact that nuclear coherence does not decay if electronic state is changed. In fact, $\gamma_{cross} = w_{21}$. This can be checked by setting isomer shift δ equal to zero. In this case electronic excitations should not affect nuclear absorption since there is no hyperfine coupling between

nuclear and electronic degrees of freedom. In this case the sum of the equations (3.9) and (3.10) yields:

$$\frac{d\left(\sigma_{31}+\sigma_{42}\right)}{dt}+i\left(\omega_{31}-\omega_{p}\right)\left(\sigma_{31}+\sigma_{42}\right)+i\Omega_{p}\left(\rho_{33}+\rho_{44}-\rho_{11}-\rho_{22}\right)= \\ -\frac{W}{2}\left(\sigma_{31}+\sigma_{42}\right)-w\sigma_{42}+\gamma_{cross}\sigma_{42}. \tag{3.13}$$

Here we used the fact that dephasing at nuclear transitions occurs only due to population decay (no inhomogeneous or homogeneous broadening of nuclear transitions), thus $\gamma_{31}=W/2$, $\gamma_{42}=\left(W+w_{21}+w_{43}\right)/2=W/2+w$, where W is the population decay rate at nuclear transitions (same for $3\rightarrow 1$ and $4\rightarrow 2$) and w is the population decay at electronic transitions (same for $2\rightarrow 1$ and $4\rightarrow 3$, formerly w_{21}). If we set $\gamma_{cross}=w$, we get that the sum $\sigma_{31}+\sigma_{42}$ behaves as if no optical driving is applied to the medium. In turn, the latter sum determines polarization excited by the probe field in nuclei. Thus, no affect of the optical field on nuclear absorptive and dispersion properties can occur, as it was expected.

Indeed, if isomer shift of levels is present, so that $\delta\neq 0$, the situation changes drastically. In order to describe possible effects of optical driving on nuclear resonant absorption, it is convenient to use dressed state picture of atomic levels. Let us neglect all relaxation processes and the presence of the probe field for a moment. In this case we are dealing with two independent two-level subsystems, namely, the transitions $2\leftrightarrow 1$ and $4\leftrightarrow 3$, interacting with strong optical field. The general form of interaction Hamiltonian between a two-level system with states $|a>$ and $|b>$ and electromagnetic field can be written as:

$$H_{2-level}=\hbar\begin{pmatrix}\Delta_{ab} & \Omega\\ \Omega^{*} & 0\end{pmatrix}. \tag{3.14}$$

Here, as usually, Ω represents Rabi frequency of the field while Δ_{ab} is the detuning

of the field from exact resonance with the transition $|a> \leftrightarrow |b>$. Diagonalizing this Hamiltonian we obtain dressed states $|\pm>$ in terms of $|a>$ and $|b>$ and the corresponding energies $E_\pm$:

$$|\pm\rangle = \frac{1}{\sqrt{1+\frac{\hbar^2\Omega^2}{E_\pm^2}}}\left(|a\rangle + \frac{\hbar\Omega}{E_\pm}|b\rangle\right), \tag{3.15}$$

$$E_\pm = \hbar\left(\frac{\Delta_{ab}}{2} \pm \sqrt{\Omega^2 + \frac{\Delta_{ab}^2}{4}}\right). \tag{3.16}$$

Let us apply this description to the 4-level electron-nuclear system. We denote dressed electronic states for the ground-state or excited nucleus as $|g_\pm>$ or $|e_\pm>$ respectively. If the driving field is in exact resonance with the electronic transition $2 \leftrightarrow 1$, the energies of the dressed states are:

$$E_{g\pm} = \pm\hbar\Omega_d \qquad E_{e\pm} = \hbar\omega_{31} + \hbar\left(\frac{\delta}{2} \pm \sqrt{\Omega_d^2 + \frac{\delta^2}{4}}\right), \tag{3.17}$$

while the corresponding states are:

$$|g_\pm\rangle = \frac{1}{\sqrt{2}}\left(|1\rangle \pm |2\rangle\right), \tag{3.18}$$

$$|e_\pm\rangle = \frac{1}{\sqrt{1+\frac{\hbar^2\Omega_d^2}{(E_{e\pm}-\hbar\omega_{31})^2}}}\left(|3\rangle + \frac{\hbar\Omega_d}{E_{e\pm}-\hbar\omega_{31}}|4\rangle\right). \tag{3.19}$$

Let us analyze these formulae. The energies of dressed states are depicted in Fig.3. We study two limiting cases: 1) low driving field intensity, $\Omega_d \ll \delta$, and 2) high driving field intensity, $\Omega \gg \delta$. In the first case the energy difference of the dressed states for the ground-state nucleus is $\hbar\Omega_d$ while for the excited nucleus this difference is $\approx \hbar\delta$. Thus, the Mössbauer absorption spectrum will consist of two pairs of resonances corresponding to the transitions $|g_\pm\rangle \rightarrow |e_-\rangle$ and $|g_\pm\rangle \rightarrow |e_+\rangle$. If Rabi frequency of the driving field Ω_d is lower than the width of the transition between the dressed states, each pair will be seen as a single line. Since the population of state

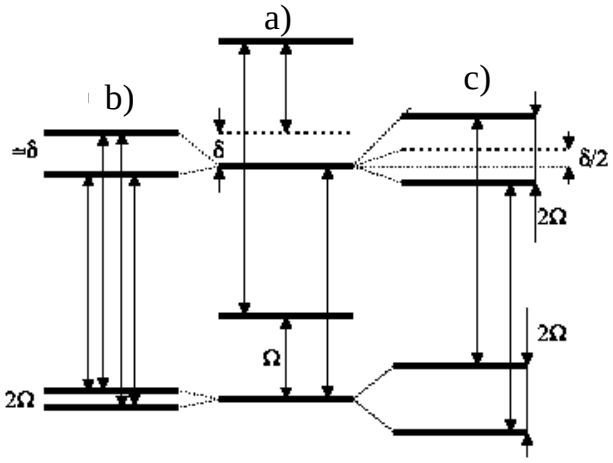

Fig. 3. Dressed state representation of the combined electron-nuclear system: a) energy state representation, b) dressed states for the case of weak driving field, and c) dressed states for strong driving field.

2 is lower than that of state 1, one pair of resonances will be weaker than the other one. In the opposite case of strong driving field the energies of dressed states for the excited nucleus are $E_{e\pm} = \hbar\left(\omega_{31} + \delta/2 \pm \Omega_d\right)$. Thus, we see that the energies of the transitions $|e_+\rangle \leftrightarrow |g_+\rangle$ and $|e_-\rangle \leftrightarrow |g_-\rangle$ become equal. These two transitions give rise to the same line in the Mössbauer absorption. As for the other two transitions between the dressed states, their dipole moments approach zero as the intensity of the driving field is increased. It can be easily checked since the dressed states for the excited nucleus become $|e_\pm\rangle = \left(|3\rangle \pm |4\rangle\right)/\sqrt{2}$ and the transitions between pairs of states 1 and 4 and 2 and 3 are forbidden. Thus, optical driving effectively decouples electronic and nuclear degrees of freedom by removing hyperfine interaction.

The complete evolution of Mössbauer spectra as the driving intensity increases is shown in Fig.4. In these calculations all relaxation processes have been taken into account. The parameters used in this calculation are given in the figure caption. However, in this calculation dephasing at optical transition was not taken into account

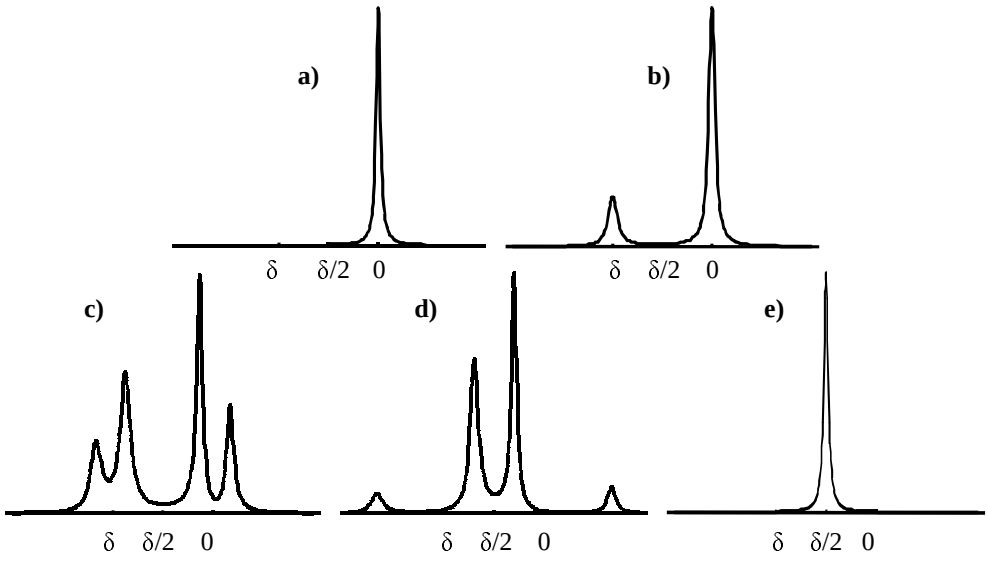

Fig. 4. Changes in the Mössbauer absorption spectrum caused by optical driving for the case of isomer shift of levels. It is assumed that $\delta \gg \gamma_{21}, \gamma_{31}$. The following situations are depicted: a) $\Omega_d = 0$ - no driving, b) $\Omega_d^2 < \gamma_{21} w_{21}$ - no saturation at optical transition, c) $\delta > \Omega_d > \sqrt{\gamma_{21} w_{21}}$ - saturated optical transition, but no cancellation of hyperfine coupling; Rabi splitting occurs, d) driving field intensity is further increased: one can see that the very left and the very right peaks go apart and drop in amplitude, while the two central peaks tend to stick together, e) $\Omega_d > \delta$ - hyperfine coupling is effectively switched off by laser driving.

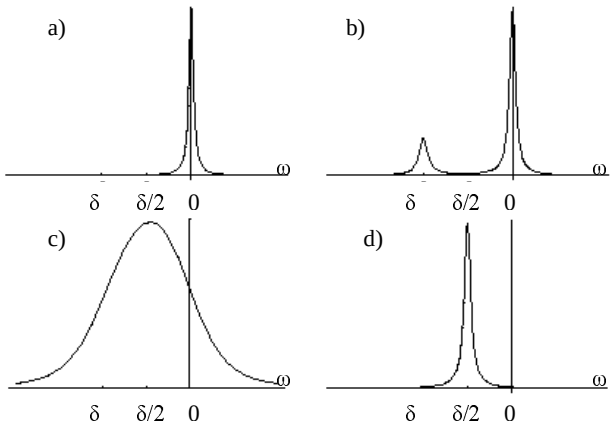

Fig. 5. Changes in the Mössbauer absorption spectrum in case of homogeneous broadening of the optical line. The following situations are depicted: a) $\Omega_d = 0$ - no driving, b) $\Omega_d^2 < \gamma_{21} w_{21}$ - no saturation at optical transition, c) $\delta > \Omega_d > \sqrt{\gamma_{21} w_{21}}$ - saturated optical transition, but no cancellation of hyperfine coupling; Rabi splitting occurs, d) $\Omega_d > \delta$ - hyperfine coupling is effectively switched off by laser driving.

so that $\gamma_{deph} = 0$. In reality this never occurs. Indeed, most optical transitions in solids are severely broadened, both homogeneously and inhomogeneously. Let us see what happens if one takes into account this broadening.

If broadening is inhomogeneous, one can affect only a small portion of all ions by means of laser driving. This portion can be calculated as $\gamma_{hom}/\gamma_{inhom}$, where $\gamma_{hom,inhom}$ are the homogeneous and inhomogeneous linewidths of optical transition respectively. This fraction gives one the portion of ions whose Mössbauer spectrum can be affected by laser. To see significant changes in the Mössbauer absorption one has to make this fraction as high as possible. The ideal situation is when all ions that give contribution to nuclear absorption are affected by optical driving field. Thus, it is preferable to work with homogeneously broadened optical lines rather than with inhomogeneously broadened ones. Let us consider how this broadening changes the evolution of Mössbauer spectra with increasing laser intensity.

If optical transition broadening is less than the isomer shift δ, the Mössbauer spectra change in exactly the same way as is depicted in Fig.4. However, in the opposite case, i.e. if $\gamma_{21} \gg \delta$, the situation changes (see Fig.5). Rabi splitting can no longer be observed since power broadening of nuclear transitions due to laser action becomes greater than isomer shift. The hyperfine structure is washed out by this broadening. However, all other stages of Mössbauer spectra evolution remain the same.

2. Hyperfine Splitting of the Ground State: Incoherent Driving

Let us now consider the case of splitting of the ground state of the electron-nuclear system. In this case some new effects can be expected. We start with the simplest ones related to population redistribution among hyperfine nuclear sublevels due to optical pumping, either coherent or incoherent.

First of all, we examine the question why ground state of the combined electron-nuclear system is so special. It is clear that either one of the four levels (see Fig.2) can be split due to hyperfine coupling, thus, giving rise to a number of Mössbauer resonances. The hyperfine structures of levels 1 and 3 can be observed without any optical driving while for observing those of levels 2 and 4 one has to optically excite a significant fraction of all ions. These effects are trivial from theoretical point of view (not from the experimental one). The only requirement for the driving field is that it should maintain sufficient population of level 2 (say, $10 \div 20\%$). However, the ground state of the system is of special interest since it does not decay. Consequently, if one manages to change population distribution among ground-state hyperfine sublevels by, say, optical means or to excite coherence between them, these changes will stay in the crystal for much longer times than for optically excited states. For example, in some rare-earth doped compounds population decay time in between the ground-state

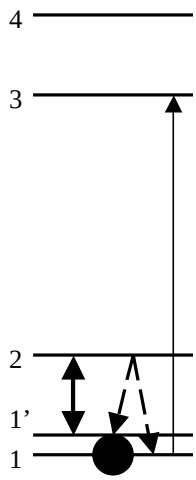

Fig. 6. Nuclear pumping via electronic excitation. Level $1'$ is depopulated and the population is stored in level 1.

sublevels can be as long as several minutes at low temperature [30].

We start considering the case of hyperfine splitting of the ground state with a possibility of redistributing ground-state population with optical radiation. Such redistribution would lead to changes in the Mössbauer spectrum of the medium. Our consideration will not involve any coherent properties of the driving optical field.

Is well known that by polarizing electrons by means of optical radiation it is possible to transfer this polarization to nuclei. This was first demonstrated both theoretically and experimentally in CaF_2 crystals doped with Tm^{2+} ions [31]. However, the degree of nuclear polarization was measured indirectly. Mössbauer experiments would allow one to check nuclear polarization in a direct manner. It was already demonstrated that nuclei can be polarized by optical means in the gaseous phase [32]. Various applications of the technique of polarizing ^3He nuclei already exist. Among them is *in vita* diagnostics of blood flow. In the following consideration we will refer to population redistribution of nuclear hyperfine sublevels as to optical pumping.

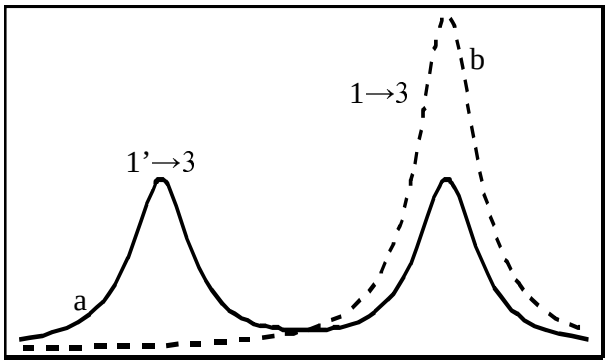

Fig. 7. Due to optical pumping of hyperfine levels $1' \rightarrow 3$ absorption is suppressed while $1 \rightarrow 3$ one is enhanced.

In order to optically pump nuclei one would have to produce spin polarization of the surrounding electrons and transfer this polarization to the nucleus by hyperfine coupling. To study this possibility we develop the following model of the combined electron-nuclear system (see Fig.6). We assume that the ground state of the system is split into two sublevels by hyperfine interaction, either magnetic or quadrupole. Than, we assume that the optical driving field can interact with only one electronic transition for the ground-state nucleus, either $1 \leftrightarrow 2$ or $1' \leftrightarrow 2$. This can be accomplished by either tuning the optical field in resonance with only one transition or by choosing right polarization of the optical field, as was done in works by Jeffries et al. [31]. As was mentioned above, typical widths of optical transitions in solids are much greater than hyperfine splittings of levels. Thus, usage of polarized light to optically pump nuclei seems more favorable.

Since the hyperfine splitting never exceeds several GHz frequencies, both ground-state hyperfine sublevels are equally populated even at low temperatures (liquid nitrogen or liquid helium). Thus, if we assume that both nuclear transitions $1 \rightarrow 3$ and $1' \rightarrow 3$ have the same strength, the unperturbed Mössbauer spectrum should look like it is shown in Fig.7, curve a. However, if the population distribution among

the sublevels is changed so that all the population is stored in level 1, one of the absorption peaks disappears while the other one gets twice as strong as without optical pumping. The disappeared absorption peak corresponds to the transition $1' \to 3$ while the other one is due to $1 \to 3$ transition.

The equations describing population redistribution among the ground-state hyperfine sublevels can be written as follows:

$$\frac{\rho_{1'1'}}{dt} + i\left(\Omega_d \sigma_{1'2} - \Omega_d^* \sigma_{21'}\right) = w\rho_{22} + w_{hf}\left(\rho_{11} - \rho_{1'1'}\right), \tag{3.20}$$

$$\frac{\rho_{11}}{dt} = w\rho_{22} + w_{hf}\left(\rho_{1'1'} - \rho_{11}\right), \tag{3.21}$$

$$\frac{\sigma_{21'}}{dt} + i\Omega_d\left(\rho_{22} - \rho_{1'1'}\right) = -\gamma_{21'}\sigma_{21'}. \tag{3.22}$$

Here w_{hf} is the population decay rate between the hyperfine sublevels. The transitions $1 \to 1'$ and $1' \to 1$ are equally probable. This reflects the fact that without optical driving both hyperfine sublevels are equally populated. Steady-state solution of the above set of equations has the following form:

$$\rho_{1'1'} = \frac{w_{hf}\left(\Omega_d^2 + \gamma_{21'}w\right)}{Z}, \quad \rho_{11} = \frac{w\Omega_d^2 + w_{hf}\left(\Omega_d^2 + \gamma_{21'}w\right)}{Z}, \quad \rho_{22} = \frac{w_{hf}\Omega_d^2}{Z}, \tag{3.23}$$

$$Z = 2\gamma_{21'}ww_{hf} + \Omega_d^2\left(3w_{hf} + w\right).$$

Here the driving field Rabi frequency was assumed real. As $\Omega_d^2 \to \infty$, the solution becomes simpler:

$$\rho_{1'1'} = \frac{w_{hf}}{w + 3w_{hf}}, \quad \rho_{11} = \frac{w + w_{hf}}{w + 3w_{hf}}, \quad \rho_{22} = \rho_{1'1'}. \tag{3.24}$$

This result can be clearly understood. The driven transition becomes saturated, thus its upper and lower levels are equally populated. However, most population is stored in level 1 under the condition of slow population decay between the hyperfine sublevels ($w_{hf} \ll w$). As one can see from the solution (3.23), efficient redistribution

of hyperfine sublevels occurs if Ω_d^2 exceeds $w_{hf}\gamma_{21'}$. This intensity is much lower than the one required to saturate optical transition.

A possibility of population redistribution of ground-state hyperfine sublevels and its detection in the Mössbauer spectrum of $^{231}Pa^{4+} : Cs_2ZrCl_6$ was discussed in our work [33]. In this work it was proposed to use circularly polarized light to pump nuclear hyperfine sublevels via interaction of optical radiation with zero-phonon line of $5f^1 \leftrightarrow 6d^1$ transition of Pa^{4+} ion. It was shown that in octahedral crystal field the selection rules for the interaction of light with atomic transitions resemble those for free atoms. In turn, optical population redistribution of hyperfine sublevels in atomic vapors is well established experimentally. The estimates of the required laser intensity give the value of W/cm^2. Such intensities are easily achievable by modern lasers.

3. Hyperfine Splitting of the Ground State: Coherent Population Trapping

Now, let us consider the case when optical field can interact with both $1 \leftrightarrow 2$ and $1' \leftrightarrow 2$ electronic transitions. Suppose that this interaction is equally strong for both transitions and that population decay rates w_{21} and $w_{21'}$ are also equal: $w_{21} = w_{21'} = w$. No population redistribution can be expected in this situation. However, a new effect of the optical field on nuclear resonant absorption can occur. It is related to so called coherent population trapping (CPT), when population of the system can be optically pumped into a coherent superposition of states non-interacting with the driving field [34]. We have to take into accout the coherence excitation between the hyperfine sublevels in a degenerate Λ-system.

Let us consider how coherence between the hyperfine sublevels can be excited and how it affects nuclear absorption. For simplicity, we choose the driving field frequency to be half the sum of the two optical transitions frequencies: $\omega_d = (\omega_1 + \omega_{1'})/2$. The

set of equations describing the behaviour of the system in the ground state of the nucleus reads as follows:

$$\frac{d\rho_{11}}{dt} + i\Omega_d\left(\sigma_{12} - \sigma_{21}\right) = w\rho_{22} + w_{hf}\left(\rho_{1'1'} - \rho_{11}\right), \tag{3.25}$$

$$\frac{d\rho_{1'1'}}{dt} + i\Omega_d\left(\sigma_{1'2} - \sigma_{21'}\right) = w\rho_{22} + w_{hf}\left(\rho_{11} - \rho_{1'1'}\right), \tag{3.26}$$

$$\frac{d\sigma_{21}}{dt} + i\frac{\delta}{2}\sigma_{21} + i\Omega_d\left(\rho_{22} - \rho_{11}\right) - i\Omega_d\sigma_{1'1} = -\gamma\sigma_{21}, \tag{3.27}$$

$$\frac{d\sigma_{21'}}{dt} - i\frac{\delta}{2}\sigma_{21'} + i\Omega_d\left(\rho_{22} - \rho_{1'1'}\right) - i\Omega_d\sigma_{11'} = -\gamma\sigma_{21'}, \tag{3.28}$$

$$\frac{d\sigma_{11'}}{dt} - i\delta\sigma_{11'} + i\Omega_d\left(\sigma_{12} - \sigma_{21'}\right) = -\gamma_{hf}\sigma_{11'}. \tag{3.29}$$

Here Ω_d, Rabi frequency of the driving field, is chosen equal for both optical transitions and real, γ is the optical transition linewidth (again, equal for both $2 \leftrightarrow 1$ and $2 \leftrightarrow 1'$), δ is the hyperfine splitting, and γ_{hf} is the linewidth of the hyperfine transition. As in the case of optical pumping, we are looking for a steady-state solution of the above set of equations. According to the assumptions, both optical transitions are completely symmetric, thus it is natural to seek for the solution in a symmetric form: $\rho_{11} = \rho_{1'1'}$ and $\sigma_{21} = -\sigma_{1'2}$. The following expressions can be obtained for populations and hyperfine coherence:

$$\rho_{22} = \frac{4\Omega_d^2\left(2\gamma_{hf}\Omega_d^2 + \gamma\left(\delta^2 + \gamma_{hf}^2\right)\right)}{Z}, \quad \rho_{11} = \rho_{1'1'} = \frac{1-\rho_{22}}{2}, \tag{3.30}$$

$$\sigma_{11'} = -\frac{2\Omega_d^2 w\left(4\Omega_d^2 - \left(\delta - 2i\gamma\right)\left(\delta - i\gamma_{hf}\right)\right)}{Z}, \tag{3.31}$$

where

$$Z = 12\Omega_d^2\left(2\gamma_{hf}\Omega_d^2 + \gamma\left(\delta^2 + \gamma_{hf}^2\right)\right) +$$
$$w\left(\delta^4 + \delta^2\left(4\gamma^2 + \gamma_{hf}^2 - 8\Omega_d^2\right) + 4\left(2\Omega_d^2 + \gamma\gamma_{hf}\right)^2\right). \tag{3.32}$$

This solution has very clear meaning as $\Omega_d \to \infty$. Under this condition it becomes

$$\rho_{22} = \frac{\gamma_{hf}}{3\gamma_{hf} + 2w}, \quad \sigma_{11'} = -\frac{w}{3\gamma_{hf} + 2w}. \tag{3.33}$$

If the condition of efficient CPT is fulfilled, i.e. if $w \gg \gamma_{hf}$, most of the population is pumped into a coherent superposition of ground-state hyperfine sublevels. This superposition does not interact with the driving field. Consequently, the absorption of the driving field is reduced and the coherence amplitude is close to maximum value 1/2.

Let us study how strong the driving field should be in order for efficient CPT to occur. Typically, $\gamma_{hf} \ll \delta$. We also assume that $\gamma_{hf} \ll w$ since this is the condition of efficient CPT. By comparing different terms in the expression for Z, we obtain that CPT is efficient if

$$\Omega_d^2 \gg \delta^2, \delta\gamma, \delta^2\gamma/w. \tag{3.34}$$

Now, we should consider the effect of the excited hyperfine coherence on nuclear absorption. In order to simplify our consideration, we assume that nuclear transitions $1 \to 3$ and $1' \to 3$ have the same absolute value of the dipole moment. Now, everything depends on the relative phase of these two moments. We consider to limiting cases: 0 relative phase and π relative phase. In the first case, dark state for the optical transitions is also a dark state for nuclear ones. Thus, the total nuclear absorption can be sufficiently reduced (see Fig.8, curve a). However, if nuclear dipole moments have opposite signs, dark state for the driving field is a bright state for γ-rays. Consequently, the absorption is enhanced rather than decreased (Fig.8, curve b). In this case the system behaves as the hyperfine interaction is removed by optical driving.

In the next chapter we discuss a possibility of observing the predicted effects

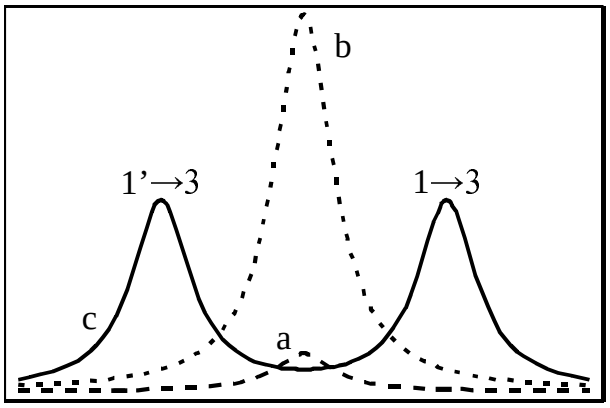

Fig. 8. Coherent population trapping due to optical driving can result in either complete suppression of nuclear absorption or in vanishing of hyperfine interaction.

in real laser-Mössbauer experiment. We discuss requirements for the medium to be satisfied in order to see changes in the Mössbauer spectrum caused by coherent optical driving. Several materials will be listed as potential candidates for the experiment.

CHAPTER IV

EXPERIMENTAL OBSERVATION OF MODIFICATIONS OF MÖSSBAUER SPECTRA BY MEANS OF OPTICAL PUMPING

In the present chapter we will discuss a possibility of experimental observation of the effects predicted above. As is clear, in order to observe modifications of nuclear resonant absorption due to resonant optical pumping, the sample under study should possess both Mössbauer-active nuclei and well-resolved electronic transitions. This places a significant restrictions on the medium to be used in the experiment. Let us start with selecting potentially suitable candidates.

A. Suitable Candidates for Experiment

Among all the elements Mössbauer effect have been detected only in 46. The most common Mössbauer isotopes are ^{57}Fe with ^{57}Co as a source and ^{119}Sn (source either ^{119}Sb or ^{119m}Sn). Approximately 90% of all Mössbauer works are related to iron. Among other Mössbauer-active nuclei are all rare-earths except for cerium (no Mössbauer transitions) and promethium (does not exist in nature), some actinides (uranium, neptunium, protactinium), many transition metals (nickel, zinc, gold, etc.), and some elements from main groups of the Periodic Table (krypton, potassium, germanium). One has to chose those of these elements possessing good optical properties (rather strong and narrow optical electronic transitions) while embedded into suitable crystalline host. It is worth to note that the host should be transparent for the optical radiation.

The elements from the main groups of the Periodic Table do not possess optically-active electrons in the outer shell, thus, they do not seem to be promising candidates for the experiment. However, all rare-earths exhibit highly-structured electronic ab-

sorption if incorporated into an optical crystal [35]. The wavelengths of the corresponding electronic transitions cover the whole optical spectral range from infrared to ultraviolet. The linewidths of these transitions depend on their origin. In the case of intraconfigurational $4f^n \leftrightarrow 4f^n$ transitions typical widths lie in the range $1 \div 100\ GHz$ and can be efficiently driven by modern lasers. However, these transitions are parity-forbidden and, therefore, are rather weak (typical oscillator strengths $\sim 10^{-6} \div 10^{-8}$). Driving of these electronic transitions would require rather high laser power. Interconfigurational $4f^n \leftrightarrow 4f^{n-1}5d$ transitions are much broader (at least, at room temperature) and much stronger (oscillator strengths can vary from 10^{-4} for spin-forbidden to 0.1 for spin-allowed transitions). They also can be efficiently driven by laser radiation. Thus, we see that optical crystals doped with rare-earth elements are potentially useful candidates for the experiment. The most common Mössbauer isotope among rare-earths is ^{151}Eu with either ^{151}Sm or ^{151}Gd source.

Actinides show similar optical properties [36] and, thus, can also be used for the Mössbauer-optical experiments. However, all of them are radioactive themselves. This would complicate the experiment a lot since intrinsic radioactivity of the Mössbauer absorber would give rise to huge background noise.

Transition metal ions in optical crystals also give rise to electronic optical transitions [37]. Even though in some cases they are not so well pronounced as in the case of intraconfigurational transitions in rare-earths, typically, they form a resolved band structure in the optical absorption at room temperature and show zero-phonon lines (ZPLs, pure electronic transitions) and structured phonon wings in low-temperature absorption and fluorescence. Thus, transition metal ions in optical crystals, such as iron and nickel, can be also considered as candidates for the laser-Mössbauer experiment.

In the following subsections we will consider several particular compounds in

more detail. The focus will be made on iron- and europium-doped optical crystals.

1. Iron-Doped Compounds

Many optical crystals containing iron ions can exhibit electronic absorption and fluorescence. The two most common valence states of iron in crystalline hosts are Fe^{2+} and Fe^{3+} even though in some compounds iron can be found in monovalent, tetravalent, and hexavalent states. We will mostly concentrate on $Fe^{2,3+}$.

Let us start with some examples of optical emission and absorption in Fe^{3+}-doped compounds. One of the most famous is tron-doped $LiAl_5O_8$ [38]. It has a spin-forbidden iron-related electronic transition in red corresponding to 658.2 nm wavelength. This transition can be efficiently excited by blue $430 \div 470$ nm or near ultraviolet $385 \div 395$ nm light. It also exhibits strong red luminescence at $660 \div 800$ nm. The fluorescence lifetime is approximately 8 ms, so that it is not hard to populate this excited state of iron ion significantly. The related compounds, namely, $Fe^{3+} : LiGa_5O_8$ [39] and $Fe^{3+} : LiAlO_2$ [40], show similar optical properties. All of them exhibit broad optical absorption and emission in near infrared at room temperature. At lower temperatures narrow zero-phonon lines and phonon structure appear in both emission and absorption. So, these crystals, if doped with enriched ^{57}Fe, would be nice candidates for the laser-Mössbauer experiment.

There are some more examples of Fe^{3+}-doped crystals possessing rather good optical properties. These are iron-doped gallium spinel $MgGa_2O_4$ emitting in red while excited in the ultraviolet [41], Fe^{3+}-doped forsterite Mg_2SiO_5 possessing electronic transition at 813 nm and having very long lifetime (≈ 15 ms) of the excited state [42], and some others. We intentionally consider only compounds consisting of rather light elements. Heavier constituents would give rise to huge off-resonant absorption of Mössbauer γ-quanta which, in turn, would complicate the prospective experiment

a lot.

Now, let us consider some compounds doped with divalent iron. The most famous Fe^{2+}-doped compounds are III-V semiconductors, such as $GaAs$, GaP, and InP (see [29] and references therein). In these materials the lowest $^5D_2$ term of Fe^{2+} ion is split into a number of electronic states by the combined action of crystal field and spin-orbit coupling. This results in a number of absorption and emission transitions in near-infrared ($2 \div 3\ \mu m$). These transitions are spin-allowed, therefore their lifetimes are much shorter than for the case of trivalent iron. At the same time, much larger oscillator strength of spin-allowed transitions makes excitation of upper electronic states easier. Thus, III-V semiconductors doped with Fe^{2+} can be also considered as potential candidates for the experiment.

In addition, it is worth to mention two other materials which iron enters in a divalent state. These are magnesium oxide $MgO : Fe^{2+}$ and $KMgF_3 : Fe^{2+}$. The former one will be considered in much greater detail in section B where the experiment on laser modification of its Mössbauer spectrum will be analyzed. Here I will discuss only optical properties $KMgF_3 : Fe^{2+}$ material. Under red excitation (kypton laser) this material emits in near-infrared $700 \div 770\ nm$ giving rise to a number of sharp ZPLs and broad phonon wing [43]. This emission originates from $^4T_1$ excited state of iron ion. This material is promising for the laser-Mössbauer experiment because the host material consists of light elements and iron-related optical transitions can be easily driven by either tunable dye or Ti:Sapphire laser.

In addition to Fe^{2+}- and Fe^{3+}-doped compounds, it is worth to mention that K_2SO_4 crystal doped with hexavalent iron (laser crystal for near-infrared range) also meets the required optical criteria. It would be extremely interesting to study the Mössbauer absorption spectrum of a lasing crystal.

2. Europium-Doped Compounds

Europium enters crystals in either divalent or trivalent state. Thus, its electronic configuration can be either $4f^6$ for Eu^{3+} or $4f^7$ for Eu^{2+}. Let us consider these two cases separately.

We start with trivalent europium ion. Its $4f^6$ electronic shell is screened from the crystalline environment by outer $5s^2$ and $5p^6$ shells as in most rare-earth ions. This fact explains why it exhibits very narrow emission and absorption lines in all optical crystals in the visible due to parity-forbidden $4f^6 \leftrightarrow 4f^6$ transitions. The typical widths of these electronic transitions are $\sim 1 \div 10\ GHz$ in ordered crystals and $100\ GHz \div 10\ THz$ in glasses [44], but in some exceptional cases the width can be as narrow as 150 MHz [45]. Eu^{3+} electronic transitions have very low oscillator strengths ($f \sim 10^{-7} \div 10^{-9}$). The ground-state level is spherically-symmetric $^7F_0$ singlet state. ^7F_J states with $J = \overline{0,6}$ extend up to 5000 cm^{-1} energies. The first excited term consists of ^5D_J states with $J = \overline{0,4}$ and extends from $\approx 17000\ cm^{-1}$ up to $\approx 27000\ cm^{-1}$. For the purpose of the laser-Mössbauer experiment the $^5D_0$ state is of the most interest for two reasons. First of all, it decays very slowly (typical lifetimes are $0.1 \div 10\ ms$) and, secondly, it can be efficiently populated via higher-lying ^5D_J states.

Some examples of Eu^{3+}-containing crystals suitable for laser-Mössbauer investigation are $Eu^{3+} : CaF_2$ with very long lifetime of $^5D_0$ state of $10 \div 13\ ms$ even at room temperature [46], europium phosphate $EuPO_4$ [47] and pentaphosphate EuP_5O_{14} [48], europium nitrate and chloride hexahydrates ($EuCl_3 \cdot 6H_2O$ and $Eu(NO_3)_3 \cdot 6H_2O$, [49]), and some others. Again, the choice of these materials was made by taking into account the fact that they should not contain heavy elements (except for europium itself) in order to avoid strong background absorption of γ-rays. All the above ma-

terials possess similar optical and Mössbauer properties. The example of optical and Mössbauer absorption spectra as well as optical emission spectrum under resonant excitation for $EuCl_3 \cdot 6H_2O$ single crystal are shown in Fig.9. In addition, Fig.10 shows calculated change in the Mössbauer spectrum if certain amount of ground-state population is placed into the excited $^5D_0$ state.

Theoretical calculation of the Mössbauer spectrum of the $^{151}Eu^{3+}$ $^5D_0$ state was carried out in the following way. First of all, one has to derive the positions of all hyperfine components of all 4 levels in Fig.2. For the ground-state nucleus hyperfine splittings are known for both $^7F_0$ and $^5D_0$ electronic states from optical measurements [45]. They originate from quadrupole interaction of the nucleus with the electronic shell. Assuming that parameters of electronic quadrupole tensor are the same for the excited nucleus and knowing the quadrupole moment for the excited-state nucleus [50], it is rather easy to evaluate hyperfine splittings for the excited nuclear states. The result of these calculations is shown in Fig.11. Secondly, one has to find relative strengths of the transitions between hyperfine components of nuclear ground and excited states for both $^7F_0$ and $^5D_0$ electronic configurations. Again, this can be easily done by calculating Clebsch-Gordan coefficients for corresponding transitions.

The situation with divalent europium-doped compounds is a little more complicated. The ground term of Eu^{2+} is $^8S_{7/2}$ ($4f^7$ electronic configuration). It contains 8 degenerate electronic states. In crystals this degeneracy is slightly lifted (see, for example, [51]), so that the energy splitting of the ground-term sublevels is of the order of several GHz. However, even at low temperature all these levels are equally populated, thus, all the states contribute to the Mössbauer spectrum. The nature of the first excited state depends on the crystal field strength. If the crystal field is sufficiently strong, so that the splitting of the $4f^6 5d$ terms is large, the lowest excited electronic state appears to be $4f^6 5d$. This happens in, for example, $Eu^{2+} : CaF_2, MgS, CaS$

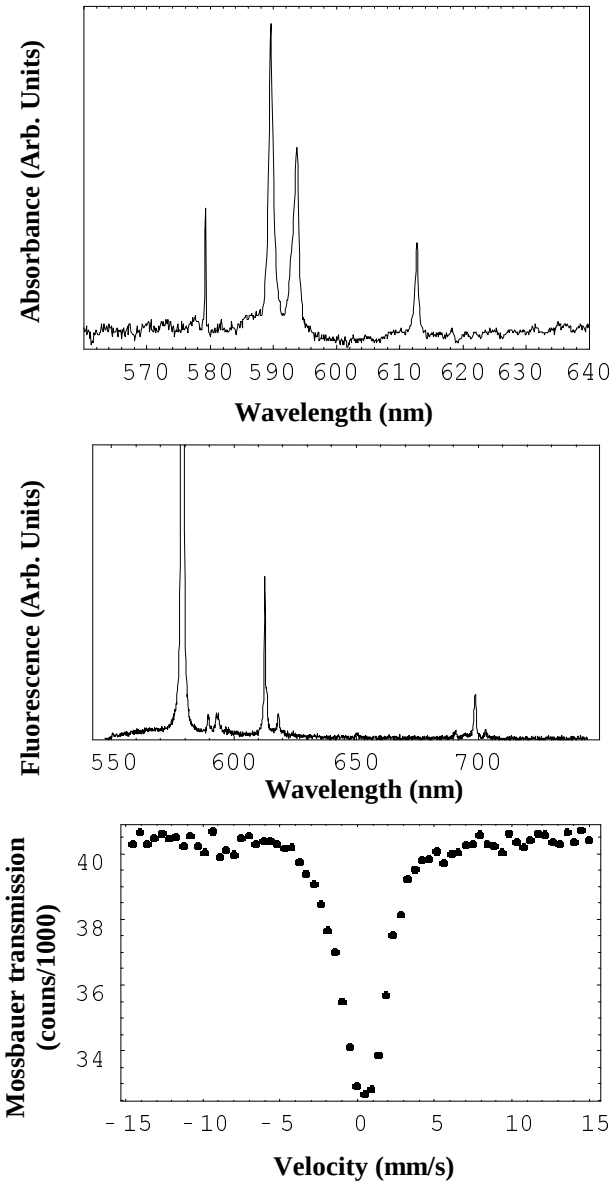

Fig. 9. Room-temperature optical and Mössbauer absorption and optical emission spectra of $EuCl_3 \cdot 6H_2O$. Optical absorption was measured in the vicinity of ${}^7F_0 \rightarrow {}^5D_0$ transition. Absorption due to thermally-populated ${}^7F_{1,2}$ levels is detected. Fluorescence was excited by a dye laser resonant to ${}^7F_0 \rightarrow {}^5D_0$ transition (579.2 nm). Multiple peaks correspond to transitions to various ${}^7F_J$ levels.

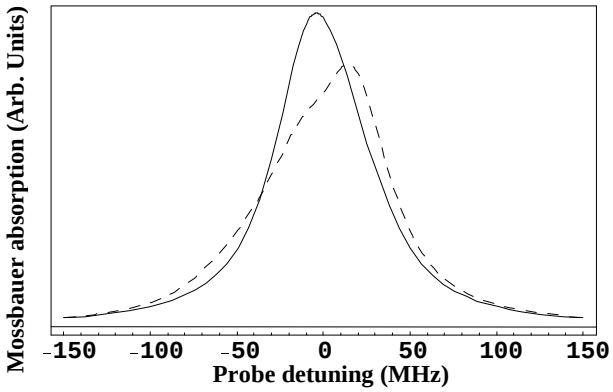

Fig. 10. Calculated Mössbauer spectra of ${}^7F_0$ (solid line) and ${}^5D_0$ (dashed line) states of $EuCl_3 \cdot 6H_2O$.

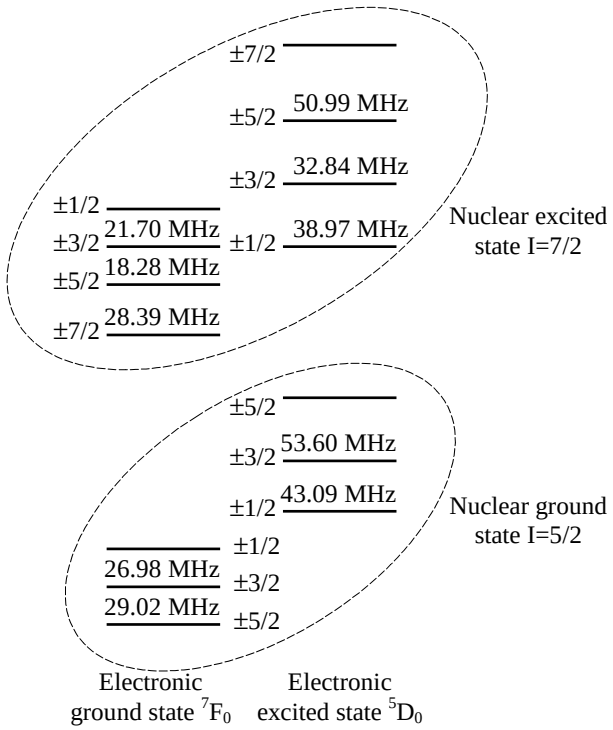

Fig. 11. Hyperfine structures of all four energy levels of ${}^{151}Eu^{3+}$ ion in $EuCl_3 \cdot 6H_2O$.

[51, 52]. The transition from the ground to the first excited state is parity allowed in this case, thus, it has very large oscillator strength ($f \sim 0.1$) and the first excited state decays very fast (lifetime is tens of nanoseconds). Using this transition one can efficiently redistribute the populations of the ground-state sublevels by polarized laser radiation (see Sec.2). However, in the opposite case of rather weak crystal field the lowest excited state of Eu^{2+} belongs to ${}^6P_{7/2}(4f^7)$ term. This situation occurs, for example, in $Eu^{2+} : KMgF_3$ material [53]. The lifetime of ${}^6P_{7/2}$ level of Eu^{2+} in $KMgF_3$ is of the order of several milliseconds. This is a very favorable situation for efficient pumping of ${}^6P_{7/2}$ metastable state via strong $4f \rightarrow 5d$ transition. Thus, $Eu^{2+} : KMgF_3$ is a very attractive material for laser-Mössbauer study.

3. Other Possible Candidates

Among the other Mössbauer-active elements the most attractive are ${}^{149}Sm$ and ${}^{169}Tm$. As all rare-earths, these two elements exhibit rather good optical properties. They both can be stabilized in either divalent or trivalent state in crystals.

Let us start with samarium. It has rather good Mössbauer properties, namely, high natural abundance of ${}^{149}Sm$ (7.38% compared to 2.12% of ${}^{57}Fe$), rather long-lived Mössbauer source ${}^{149}Eu$ (half-life time 93.1 days), and high probability of populating the excited Mössbauer state of ${}^{149}Sm$ nucleus (64%, [50]). The ${}^{149}Eu$ source can be produced by ${}^{150}Sm(p, 2n){}^{149}Eu$ reaction [54].

Trivalent samarium can be studied in many host materials. The examples of optical properties of Sm^{3+} ion incorporated into CaF_2 and of Sm_2O_3 are given in Refs.[55] and [56]. Excitation of electronic states can be accomplished by dye laser at $\approx 570\ nm$.

Divalent samarium has the same ground-state electronic configuration as Eu^{3+}, namely, $4f^6$. However, the distinction between these two ions comes from the fact

that the lowest $4f^5 5d$ term of samarium lies either in the visible or in the near UV. Consequently, two different situations can occur. First of all, the lowest $5d$ level can lie below metastable $^5D_0$ state. This happens in CaF_2 doped with Sm^{2+} [57]. However, in some materials, for example, in SrF_2, the lowest $5d$ state lies above metastable $^5D_0$. This would allow one to efficiently pump $^5D_0$ level via higher-lying $4f^5 5d$ levels. The situation is similar to the case of $Eu^{2+} : KMgF_3$ considered in Sect.2.

Now, let us turn to thulium-doped compounds. The advantages of this element are 1) 100% natural abundance of Mössbauer isotope ^{169}Tm and 2) low energy of Mössbauer transition (8.41 keV). However, shortcomings are more extensive. First of all, ^{169}Tm has very broad Mössbauer linewidth corresponding to the excited state lifetime ≈ 4 ns. Secondly, radioactive Mössbauer sources are very short-lived (9.4 days for ^{169}Er and 32 days for ^{169}Yb), thus, making conventional Mössbauer experiment very complicated. The best choice for ^{169}Tm-doped compounds would be laser-Mössbauer experiment at synchrotron Mössbauer source [58]. The most advantageous material to be used in this experiment is $Tm^{2+} : CaF_2$ because of its electronic-level structure. Tm^{2+} in CaF_2 exhibits absorption in the visible due to parity-allowed $4f^{13} \leftrightarrow 4f^{12}5d$ transition. From $5d$-state population decays very efficiently to the metastable $4f$ state situating 8966.2 cm^{-1} above the ground-state level [59]. Again, as in the case of $Eu^{2+} : KMgF_3$ metastable state can be efficiently populated and its hyperfine structure can be studied by means of Mössbauer spectroscopy. Furthermore, $Tm^{2+} : CaF_2$ is laser material (see [60]), thus, it is possible to observe Mössbauer spectrum of a lasing crystal.

Laser-Mössbauer experiment can be also performed with some other elements, such as, for example, nickel and dysprosium. However, additional search of literature is needed to conclude about feasibility of such an experiment.

4. Estimates for Required Laser Intensities

Let us now estimate the laser intensity required to observe the effects discussed in Chapter III. We start with a simple energetical consideration based on how much laser power is required to populate the upper electronic state.

Typical optical transitions in solids are within the wavelength range $100 \div 1000\ nm$. The corresponding energy of a photon is of the order of a few eV. Let us take $2\ eV$ for electronic excitation. This means that in order to excite one ions just once, about $3 \times 10^{-19}\ J$ of energy is needed. In order to collect good-quality Mössbauer spectrum, nuclear resonant absorption should be of the order of 10%. This is enough to observe pronounced nuclear resonances without thickness broadening. Nuclear resonant cross-section for ^{57}Fe is $2.5 \times 10^{-18}\ cm^2$, for europium-151 it is a bit less. Thus, in order to see 10% of nuclear absorption, $4 \times 10^{16}\ ions/cm^2$ is required. Consequently, if one expects to see 20% of change in the Mössbauer spectrum due to optical excitation, about $10^{16}\ ions/cm^2$ should be excited by a laser. For the conventional Mössbauer spectroscopy the required aperture is $\sim 0.1 \div 1\ cm^2$. Thus, we need $\sim 10^{15} \div 10^{16}$ ions in the excited state in order to observe significant changes in nuclear absorption. This means, that in order to produce significant population of the excited electronic state, one needs $E_{ex} \sim 0.3 \div 3\ mJ$ of energy.

The above estimate does not seem something unachievable. However, one needs to remember that typical Mössbauer experiments last for several hours and even days. Thus, it is required to maintain the population of the upper electronic state for a time much longer than its lifetime. The required power can be estimated simply as E_{ex}/τ with τ being the lifetime of the excited electronic state. The typical lifetimes for electronic transitions in transition-metal ions are in the range from several microseconds (for spin-allowed transitions) to several milliseconds (for spin-forbidden transitions).

Thus, the power required to maintain the population of the excited electronic state is within the range from several hundred milliwatts to several watts for spin-forbidden electronic transitions and much higher for spin-allowed ones. Thus, in order to see changes in nuclear absorption related just to population of the excited electronic state, rather powerful laser is required. Such a big power would heat the Mössbauer absorber a lot and one has to take special precautions to avoid sample overheating and destruction of the Mössbauer effect conditions.

For ^{151}Eu the situation is even worse than it is for iron. It is the experimental fact that one needs at least 10^{19} $ions/cm^2$ to collect a good-quality Mössbauer spectra of europium. The lifetime of the metastable $^5D_0$ state of Eu^{3+} is typically in the millisecond range. Thus, in order to maintain the population of the excited $^5D_0$ level, the laser power should be very high - hundreds watts or even kilowatts. Such a huge power will definitely destroy the crystal. For instance, for the above example of $EuCl_3 \cdot 6H_2O$ the laser power required to excite several tens per cent of Eu^{3+} ions is roughly 1 kW/cm^2. This result should have been expected since typical saturation powers for $4f \leftrightarrow 4f$ transitions in rare-earth-doped crystals are of the same order.

It is clear, that in order to observe coherent effects in nuclear absorption, much higher powers are needed. Thus, we see that only incoherent effects related to the excitation of rather metastable (with lifetimes of several milliseconds) states can possibly be observed in a conventional Mössbauer experiment. The question arises: what can be done to improve the situation and to make the observation of the predicted laser-induced effects possible? There are at least two ways to do it.

The first way is to try to reduce the aperture required for Mössbauer measurements. For the conventional Mössbauer spectroscopy this means simultaneous decrease in γ-quanta counting rate. There is a trade-off between the laser power and the time required to collect the spectrum. If, for example, the Mössbauer aperture

is reduced ten times, we need ten times less laser power, but, simultaneously, we need to collect the Mössbauer spectrum ten times longer. However, there is a way to avoid this trade-off by using a synchrotron Mössbauer source [61]. The advantage of working with synchrotron Mössbauer source is that synchrotron radiation is very well collimated. Its divergence can be as low as μrad. Furthermore, it can be focused down to a 5 μm-diameter spot [62]. With this tight focusing the requirements for laser power drop dramatically. For example, in case of $EuCl_3 \cdot 6H_2O$ crystal instead of kilowatt laser powers one would need only several milliwatts focused to ~ 10 μm spot to produce substantial population of $^5D_0$ state.

Synchrotron Mössbauer sources exist for several Mössbauer element: $Tm - 169$, $Eu - 151$, $Dy - 161$, $Fe - 57$, $Sm - 149$, etc. Thus, the crystals doped with these elements can be considered as good candidates for laser-synchrotron experiments.

Another way to avoid difficulties related to laser-power requirements is related to synchronization of the laser action with the emission of a γ-photon. Previously we considered the case in which the system prepared in some electronic state or in coherent superposition of states waits for the γ-photon to come. This is required since γ-photons are emitted randomly by the Mössbauer source. Let us consider what happens if we know exactly when the excited state of the source is formed. Than, we should expect the Mössbauer photon to come to the detector within the nuclear lifetime. Consequently, we can illuminate the sample for a rather short period of time (100 ns in case of ^{57}Fe) with a pulsed laser and we do not need to continue illumination after this period of time. This opens a possibility to do laser-Mössbauer experiments with short-lived electronic states (with lifetimes comparable to the nuclear one or longer). Furthermore, peak intensities of laser pulses are high enough to observe coherent effects, such as Rabi-splitting of Mössbauer lines.

How do we know when the excited nuclear state of the source nucleus is formed?

For ^{57}Fe the time of the excited nuclear state formation can be determined in the following way. 14.4 keV nuclear state is not populated directly from ^{57}Co β-decay, but through an intermediate 136 keV state of ^{57}Fe. The population of 14.4 keV state is accompanied by the emission of 122 keV photon. Thus, if at some instant of time we detect this photon, we immediately know that the source will emit 14.4 keV Mössbauer photon within the next 100 ns. This time is enough to make the laser generate a pulse of optical radiation. This method is called coincidence technique. It is widely used in nuclear physics. Unfortunately, it is not that simple to implement coincidence technique for other Mössbauer isotopes.

B. Modification of Mössbauer Spectrum of $^{57}Fe^{2+} : MgO$

In this section experimental observation of laser-induced changes in the Mössbauer absorption of $^{57}Fe^{2+} : MgO$ will be discussed [63].

1. Literature Overview

Magnesium oxide crystal doped with divalent iron has been studied a lot. Both Mössbauer and optical investigations have been carried out by different groups of scientists. Let us start with review of optical properties of this crystal.

Undoped magnesium oxide has octahedral crystal structure similar to that of $NaCl$. Iron can enter this crystal in magnesium sites in either divalent state or in trivalent state with charge compensation. It is rather easy to switch between divalent and trivalent iron by firing the crystal sample in either reducing or oxidizing atmosphere respectively. The site of divalent iron ion incorporated into MgO has octahedral symmetry. Thus, the crystal field cannot remove the degeneracy of electronic levels completely. The first works in which electronic states of $3d^6$ ions in octahedral

symmetry were studied both theoretically and experimentally were Refs.[64]. In these works it was shown that the ground-state $^5D_2$ term of such ions is split by the crystal field into T (lower one) and E (upper one) manifolds. The T manifold contains 15 electronic states while the remaining 10 electronic states of $^5D_2$ configuration belong to E manifold. The consequent spin-orbit splitting of these two manifolds lifts the degeneracy further. However, the degeneracy is not removed completely because of high symmetry of octahedral crystal field. Further removal of electronic degeneracy can be accomplished by adding distortions of lower symmetry to the crystal field due to imperfections of the crystal or due to electron-phonon coupling (Jahn-Teller effect). The overall structure of electronic levels is similar to that of Fe^{2+} in III-V semiconductor compounds [29]. All the distinctions are of quantitative character because of different crystal field coupling (different $10Dq$) and different spin-orbit coupling parameter λ.

Low temperature optical absorption spectra of $MgO : Fe^{2+}$ have been studied by many authors [65]. It is well-known that the optical absorption spectrum of $MgO : Fe^{2+}$ consists of a sharp zero-phonon line corresponding to the electronic transition to the ^5E_g state located at $\approx$ 9350 cm^{-1} and a wide phonon sideband spreading up to 14000 cm^{-1}.

Mössbauer studies of $MgO :^{57} Fe^{2+}$ were primarily focused on Jahn-Teller effect present in this crystal at low temperatures. It is known, that cubic symmetry of Fe^{2+} site in MgO is distorted by random strains at nuclear site [66] giving rise to quadrupole splitting of ^{57}Fe Mössbauer transition. However, fast relaxation processes between ground-state electronic sublevels remove this splitting at temperatures higher than 14 K. Relaxation rates strongly depend on the positions of electronic levels. In turn, the positions of all levels are dependent on dymanic Jahn-Teller effect. Theoretical description of relaxation effect on quadrupole splitting in the Mössbauer

spectra was developed by Ham [67].

2. Sample Preparation

The sample of $^{57}Fe^{2+} : MgO$ for the laser-Mössbauer experiment was prepared in the following way. A MgO substrate was purchased with MTI Corp. It was covered with a thin layer of $^{57}Fe_2O_3$ (95% enrichment, purchased with Matech) and fired in air for a week at $\approx 750^oC$. The resulting crystal contained small amount of divalent iron in cubic symmetry. However, much greater amount of iron formed ferrites. This fact was checked by observing broadened sextets in the room-temperature Mössbauer absorption (see Fig.12a). To reduce ferrite content, the sample was annealed for ≈ 20 hours at 1100^oC in hydrogen atmosphere. The hydrogen was obtained by electrolysis of $NaCl$ solution and purified by passing it through a copper tube immersed in liquid nitrogen. After annealing dark-green-blue sample was obtained. The geometrical dimensions were $10 \times 10 \times 0.5\ mm^3$. The resulting crystalline sample contained no ferrite showing only the presence of divalent iron in cubic symmetry (see Fig.12b). However, Fe^{2+} surrounding was distorted. This resulted in rather broad Mössbauer line and in splitting of a cubic singlet into two lines due to random strains.

3. Experimental Arrangement

The experimental setup diagram is shown in Fig.13. The sample of $MgO :^{57} Fe^{2+}$ is placed in between the moving Mössbauer source and γ-photon counter. The Mössauer source used in the experiment was $^{57}Co : Rh$, the Mössbauer spectrometer was from Wissel Instruments, and the detector was a simple proportional counter. The initial source activity was $\approx 50\ mCi$, however, by the time when the experiments were performed it dropped to $10 \div 15\ mCi$. The Mössbauer counting rates in the experiments varied in the kilohertz range.

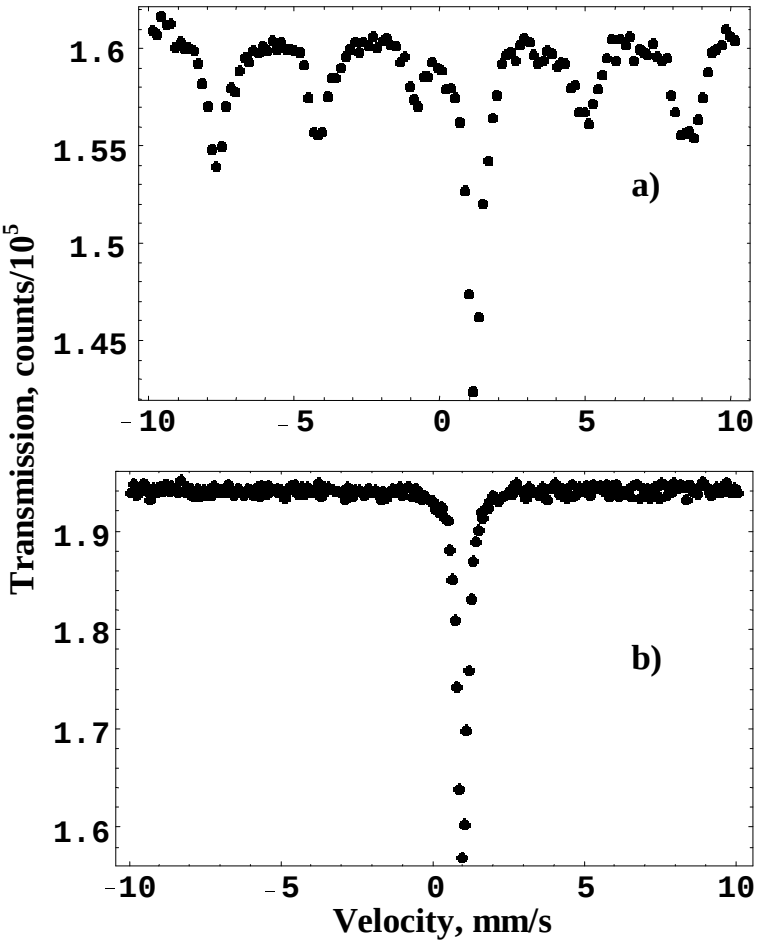

Fig. 12. Room-temperature Mössbauer spectra of $^{57}Fe : MgO$ after the diffusion and after consequent reducing in H_2 atmosphere. Non-reduced sample showed rich ferrite structure of $^{57}Fe^{3+}$ while the reduced sample contains only Fe^{2+}.

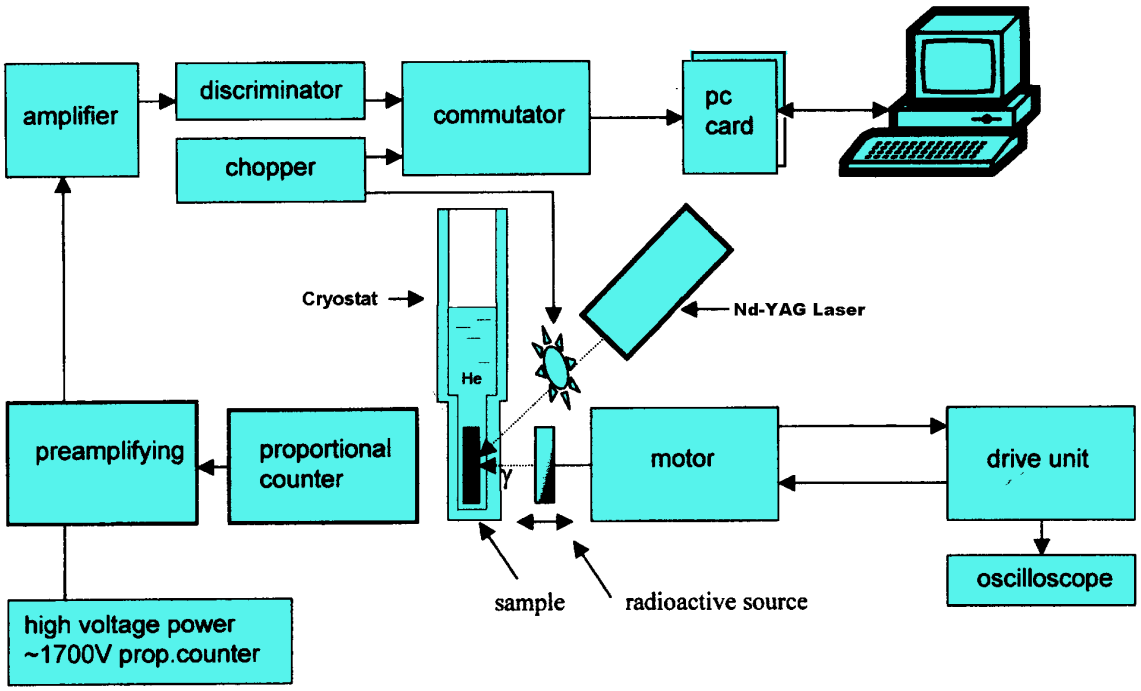

Fig. 13. Setup for laser-Mössbauer experiment.

Two different lasers were used to illuminate the absorber. One of them, $Nd:YAG$ laser was an old ESI3570 manufactured in $\approx$ 1985. It was capable to deliver up to 30 W of CW power at 1064 nm. It also could be Q-switched. The Q-switch rates could vary from a single pulse up to 20 kHz in steps of 100 Hz. The pulse duration could be either 35 ns or 70 ns depending on the laser cavity length. The average power in a Q-switch mode dropped by approximately a factor of 3. The laser beam was directed onto the sample by passing it through a KTP doubling crystal to visualize a beam. Only a small fraction of laser power was converted into 532 nm second harmonic.

The second laser used in the experiments was GM30 $Nd:YLF$ laser from Photonics Industries. This laser was capable of delivering of ≈ 1 W of green power (527 nm) in CW regime, while in the Q-switch mode the average power could be made as high as 30 W. The repetition rates could be varied in the range 600 $Hz \div 3$ kHz. The pulse duration was dependent on the repetition rate and pump power. Typical pulse widths lied in the range 150 ns for high pump power through 1 μs for low pump power.

The laser beam was focused onto the sample to a spot $\approx 3 \div 4$ mm in diameter corresponding to the apperture used in the Mössbauer experiment. To avoid overheating of the sample, it was placed on a massive copper holder. To improve thermal contact of the sample with the holder, thermo-conducting greeze was used.

For low-temperature measurements the sample was placed into a cryostat (ST-100, Janis Research). Fluorite (CaF_2) windows were used for passing the laser beam while γ-rays were passed through mylar Mössbauer windows. The sample was mounted on a "cold finger".

As was mentioned above, Mössbauer spectra are very sensitive to the absorber temperature. In particular, isomer shift of the Mössbauer lines and quadrupole split-

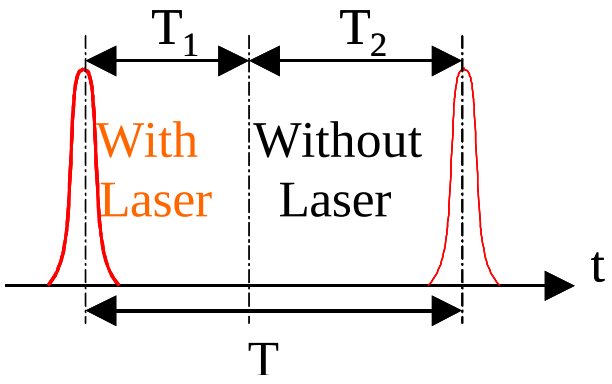

Fig. 14. Mössbauer data collection procedure.

ting depend very strongly on the temperature: they decrease as the sample is heated up. Significant changes of isomer shift and quadrupole splitting can be detected if the sample temperature is changed by $\sim 10\ K$. However, laser radiation can heat the sample by several tens or even hundreds K. To avoid misleading results caused by laser heating, one has to accumulate the Mössbauer spectra with laser on and off at the same sample temperature. Thus, the Mössbauer spectra were collected in the following way. The period of time between the two subsequent laser pulses was split into two parts. γ-quanta detected during each part of the period formed different Mössbauer spectra. Thus, two spectra were obtained simultaneously. The spectrum collected during the first part of the period between pulses was called "with laser" while the spectrum corresponding to the second part of the period was called "without laser" (see Fig.14). In fact, words "with laser" and "without laser" do not reflect the real situation because both spectra were taken with no laser light on. "With laser" means right after the laser pulse and "without laser" means right before the next laser pulse. If laser causes some excitation (for example, some electronic excitation) inside the crystal whose lifetime is of the order of laser repetition period, the two Mössbauer spectra taken "with" and "without laser" should be different (of course, if

this excitation affects nuclear hyperfine properties). So, one has to accumulate these two spectra and compare them.

Let us estimate the maximum temperature increase that might be caused by a laser pulse. This is necessary in order to check the expected thermal effects. The laser pulse energy in the experiments with $^{57}Fe : MgO$ did not exceed $1 - 3\ mJ$. Let us assume that all this energy goes into heat. We also assume that all this heat is dissipated during the "with laser" part of the laser period. This will give us the upper estimate of the sample temperature difference between "with" and "without laser" periods of time. We also assume that only the illuminated area is heated up. Thus, the heated volume in the case of our $^{57}Fe : MgO$ sample is $3 \times 3 \times 0.5\ mm^3$. The density of MgO is $3.6\ g/cm^3$ while its specific heat capacity is $0.94\ J/(g \cdot K)$. Taking into account all these data, we obtain $0.2\ K$ utmost temperature difference for the two parts of laser period. Such small temperature difference cannot cause any measurable changes in the Mössbauer absorption of the sample.

4. Experimental Results

Before discussing the changes in the Mössbauer spectrum by laser radiation, it is necessary to present both Mössbauer and optical spectra of the sample under study. The room temperature optical absorption of our blue-green sample is shown in Fig.15. It shows several broad bands in the visible and infrared parts of the spectrum. These bands are peaking at $\sim$ 8000 cm^{-1}, 16000 cm^{-1}, and 18000 cm^{-1}. There is also strong absorption in the violet.

The results of Mössbauer studies of the sample are shown in Fig.16. Mössbauer spectra were taken at different temperatures, from liquid nitrogen up to room temperature. Divalent iron occupies octahedral sites in MgO, thus high-symmetry crystal field cannot lead to quadrupole splitting of nuclear levels. Consequently, Mössbauer

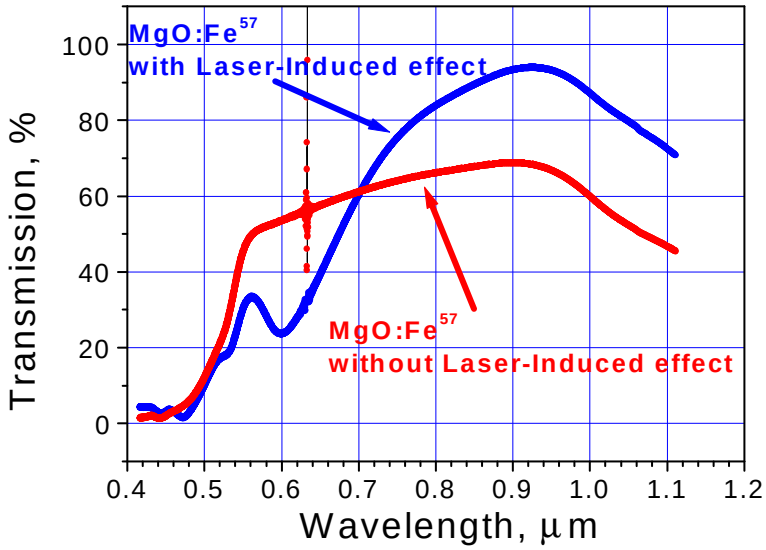

Fig. 15. Optical absorption of the two samples of $^{57}Fe^{2+} : MgO$. The one in which laser-induced effect is observed has pronounced absorption peaks at $\approx 530\ nm$ and $\approx 600\ nm$. Peak at $632\ nm$ is due to $He - Ne$ calibration laser.

spectrum should consist of one line. However, random strains inside the crystal lower the site symmetry. Fig.16 shows that Mössbauer absorption of our sample is not a single line but rather a quadrupole doublet. As the temperature is increased, quadrupole splitting decreases and the absorption line becomes sharper. This indicates the fact that relaxation processes are involved in forming the Mössbauer line shape. The relaxation effects in the Mössbauer spectrum of the sample under study will be discussed in the next subsection.

In laser-Mössbauer experiments two types of lasers were used: fundamental and second harmonics of $Nd : YAG$ (1064 nm and 532 nm respectively) and second harmonic of $Nd : YLF$ (527 nm). Let us start with 1064 nm pumping experiments.

The typical difference between "with" and "without laser" spectra is shown in Fig.17. This figure also shows the way in which the change in the Mössbauer spectra is measured. Namely, the sum of areas of positive and negative parts of difference

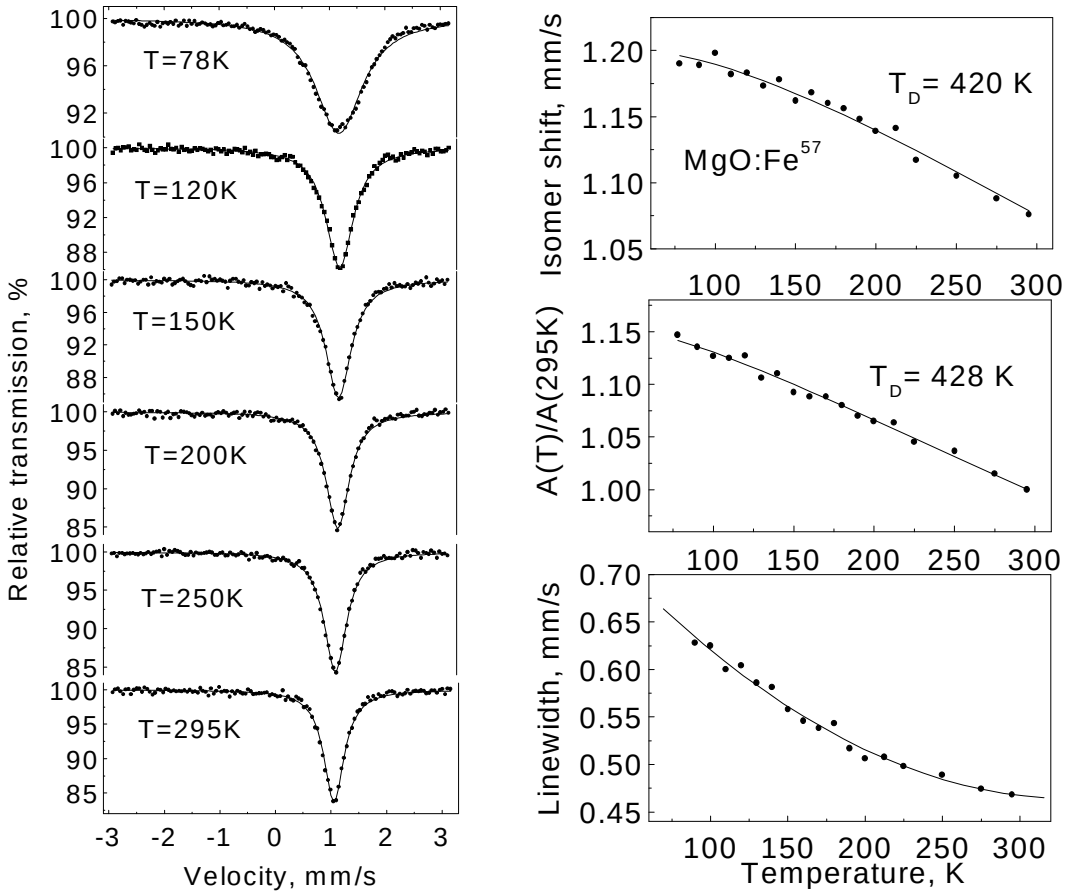

Fig. 16. Temperature dependence of $^{57}Fe^{2+} : MgO$ Mössbauer spectra. The dependences of absorption area and isomer shift on T allows one to estimate the Debye temperature ($\Theta_D \approx 420\ K$). Relaxation effects lead to narrowing of the Mössbauer line as the temperature is increased.

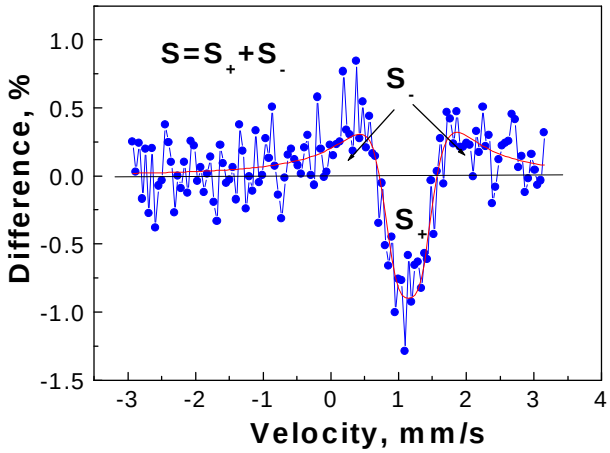

Fig. 17. Measure of laser-induced effect as a sum of areas of positive and negative parts of spectral difference.

between "with"- and "without laser"-spectra was chosen as a measure of "laser effect". Its dependence on the acquisition time T_1 is indicated in Fig.18. Even though there are only four points in this graph, it is possible to determine the order of magnitude of "laser effect" lifetime: $\sim$ 100 μs. The maximum amplitude in the Mössbauer absorption difference observed in the experiments with $Nd:YAG$ laser was $\approx 2\%$.

Much better results are obtained with 527 nm pumping. With the same optical power it is possible to affect Mössbauer absorption three times more efficiently. The typical spectra of $^{57}Fe^{2+}:MgO$ under laser action are shown in Fig.19. In that experiment the pulse repetition rate was 2.9 kHz and "with/without laser" parts of the repetition period were equal. As in the case of $Nd:YAG$ pumping, the dependence of "laser effect" was studied as a function of acquisition time T_1 (see Fig.20). This time the difference in maxima of "with/without laser" Mössbauer absorption was chosen as a measure of "laser effect". The parameters of laser radiation used in this series of experiments are the following: power 3.25 W, pulse repetition rate 2.5 kHz, and pulse duration 650 ns. The experimental points were fitted in the following way.

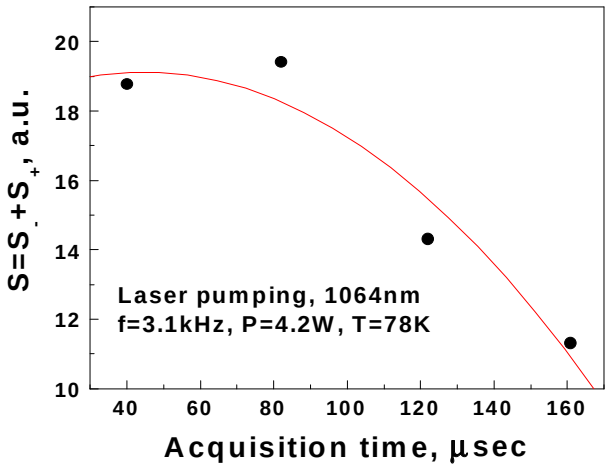

Fig. 18. Acquisition time dependence of laser-induced effect in case of $Nd : YAG$ pumping.

Let us assume, that the change produced by a laser pulse inside the crystal decays exponentially. Thus, the parameter describing this change behaves as

$$f(t) = ae^{-t/\tau}, \tag{4.1}$$

where a is the initial amplitude of change right after the pulse and τ is its lifetime. What is observed in the experiment is the difference between values of $f(t)$ averaged over "with" and "without laser" parts of the period:

$$\overline{\Delta f(t)} = \frac{1}{T_1}\int_0^{T_1} f(t)dt - \frac{1}{T-T_1}\int_{T_1}^{T} f(t)dt, \tag{4.2}$$

where T is the pulse repetition period. Evaluating this expression we obtain the following formula for the difference in Mössbauer amplitude for "with/without laser" parts of the repetition period:

$$\Delta A = X\left[\frac{T}{T_1}\left(1 - e^{-\frac{T_1}{T}\frac{T}{\tau}}\right) - \frac{T}{T-T_1}\left(e^{-\frac{T_1}{T}\frac{T}{\tau}} - e^{-\frac{T}{\tau}}\right)\right]. \tag{4.3}$$

This expression contains only three parameters: X is the amplitude, T_1/T is the

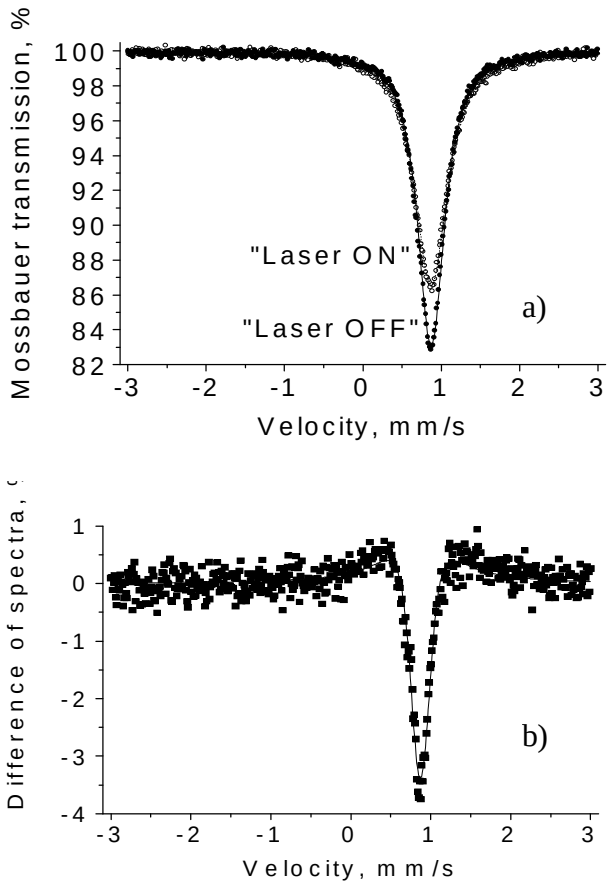

Fig. 19. Room-temperature laser-induced effect in $^{57}Fe^{2+} : MgO$ with $\approx 4.5\ W$ pumping at 527 nm ($Nd : YLF$, second harmonic) and the repetition rate 2.9 kHz: a) spectra "with/without laser" ("laser on/off"), b) the difference of the two spectra.

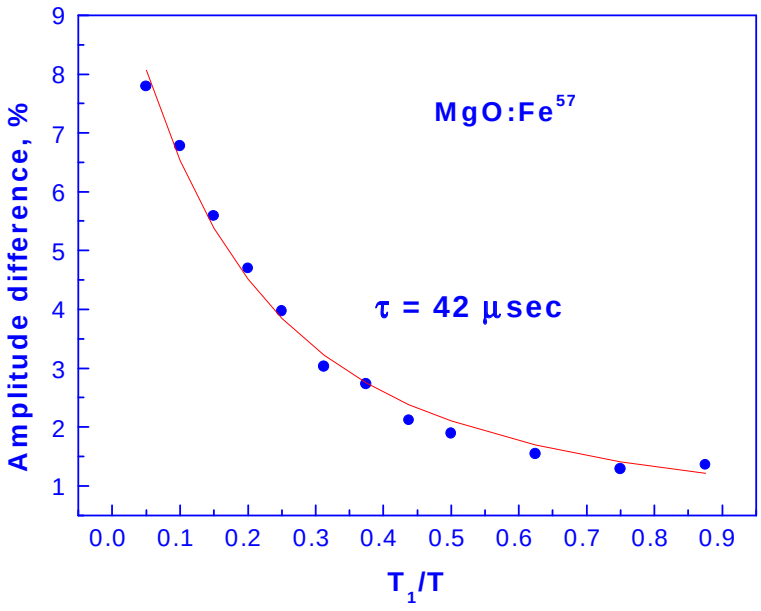

Fig. 20. Acquisition time dependence of laser-induced effect amplitude. Fitting gives the lifetime $\approx 40\ \mu s$.

fraction of "with laser" part, and τ/T. By fitting the experimental points with this curve it is possible to determine the lifetime of laser-induced changes: $\tau = 40\ \mu s$. This is of the same order as our previous estimate $\sim 100\ \mu s$ done for $Nd : YAG$ experiments.

In addition to substantial change in the amplitude (for T_1 less than 40 ns the amplitude dropped more than twice) and broadening of the Mössbauer line, additional Mössbauer absorption resonances were observed for acquisition time T_1 less than 40 ns (see Fig.21). They might originate from the hyperfine structures of the excited electronic states of $^{57}Fe^{2+}$ ion.

In order to check weither the observed changes in the Mössbauer spectrum are really related to laser action, several experiments with other samples were done. These samples were Al_2O_3 :^{57} Fe^{3+} and $MgAl_2O_4$:^{57} Fe^{3+}. They were prepared by iron diffusion into the host material at high temperatures: 900^oC for Al_2O_3 and 1200^oC

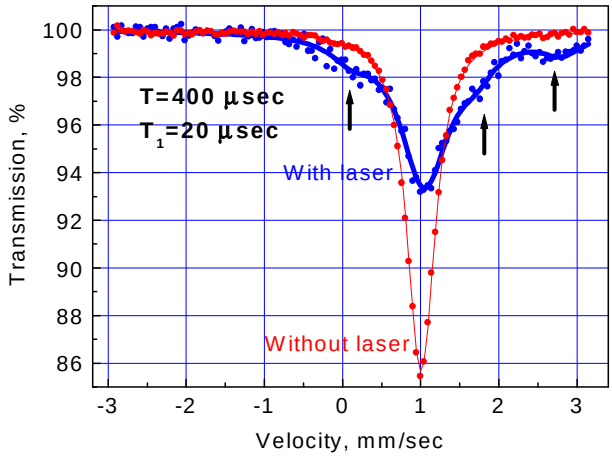

Fig. 21. Room-temperature laser-induced effect in $^{57}Fe^{2+} : MgO$ with $\approx 3.25\ W$ pumping at 527 nm ($Nd : YLF$, second harmonic) at the repetition rate 2.5 kHz and acquisition time $T_1 = 20\ \mu s$. Additional Mössbauer resonances are indicated by arrows.

for spinel. The geometrical dimensions of the latter two samples were identical to those of blue-green $MgO : Fe$. In Fig.22 a comparison of laser-induced effect for the same laser parameters is shown. No effect can be seen for corundum and spinel while it is very pronounced for magnesium oxide.

In order to check that the produced sample of $MgO :^{57} Fe^{2+}$ is not unique and that the procedure of its preparation is repeatable, one more sample of $MgO :^{57} Fe^{2+}$ was produced following the procedure described above. However, this time the hydrogen was not purified in liquid nitrogen. This resulted in more pronounced quadrupole splitting (see Fig.23). Probably, this was caused by lowering iron site symmetry due to impurities. The produced sample was much more transparent than the first one. No changes in the Mössbauer spectrum under laser irradiation were observed.

The third sample of $MgO :^{57} Fe^{2+}$ was reduced in a purified hydrogen at 900^oC. It appeared to be more transparent as the first one (no blue-green coloration). In

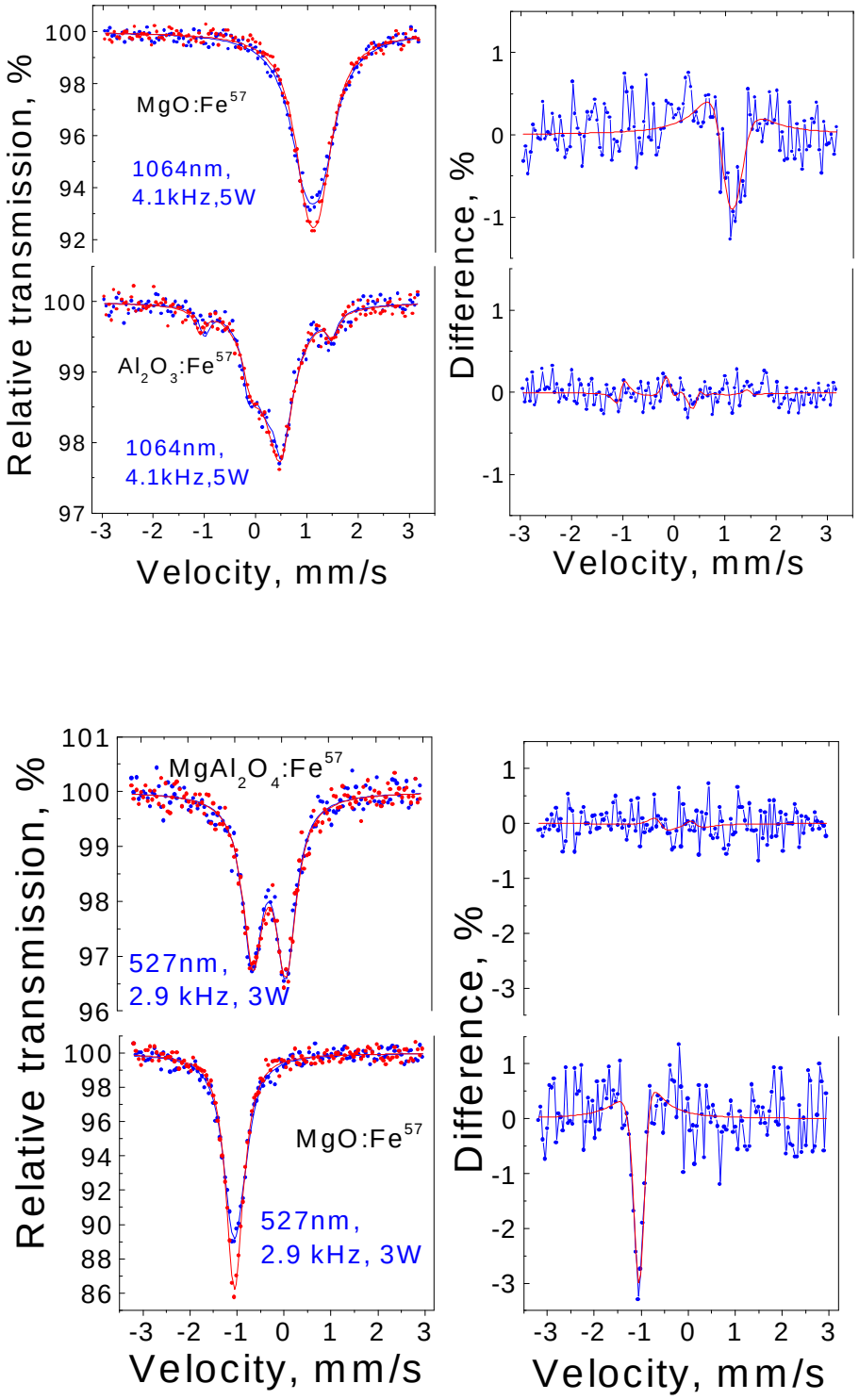

Fig. 22. Comparison of laser-induced effect in different samples: a) $^{57}Fe^{2+} : MgO$ vs. $^{57}Fe^{3+} : Al_2O_3$ and b) $^{57}Fe^{2+} : MgO$ vs. $^{57}Fe^{3+} : MgAl_2O_4$.

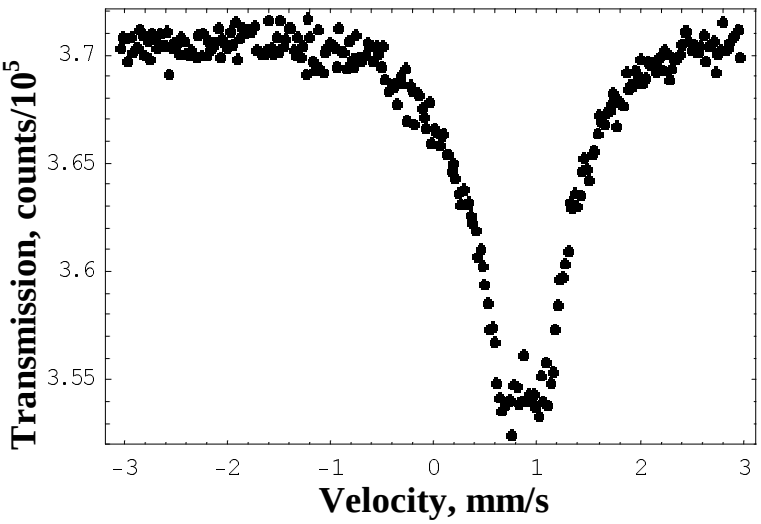

Fig. 23. Mössbauer spectrum of $^{57}Fe^{2+} : MgO$ sample reduced in impure hydrogen. No laser-induced effect is detected.

addition, it contained substantional amount of ferrite. Even though it looked completely different from the first dark green-blue sample, its Mössbauer spectrum was affected by laser radiation (see Fig.24). Thus, the conclusion is that the procedure of producing $MgO :^{57} Fe^{2+}$ crystals, whose Mössbauer spectrum can be affected by 527 nm radiation, exists and repeatable.

5. Possible Explanations of Observed Changes

Even though no satisfactory explanation of the observed modifications of Mössbauer spectrum exists so far, one can speculate about possible origin of these modifications. Let us discuss possible explanations of the observed effect. The two facts have to be explained: appearance of new Mössbauer resonances and broadening of the initial line.

In section 3 of the present chapter possible thermal effects were already estimated. Possible change in temperature by 0.2 K could not lead to such a strong

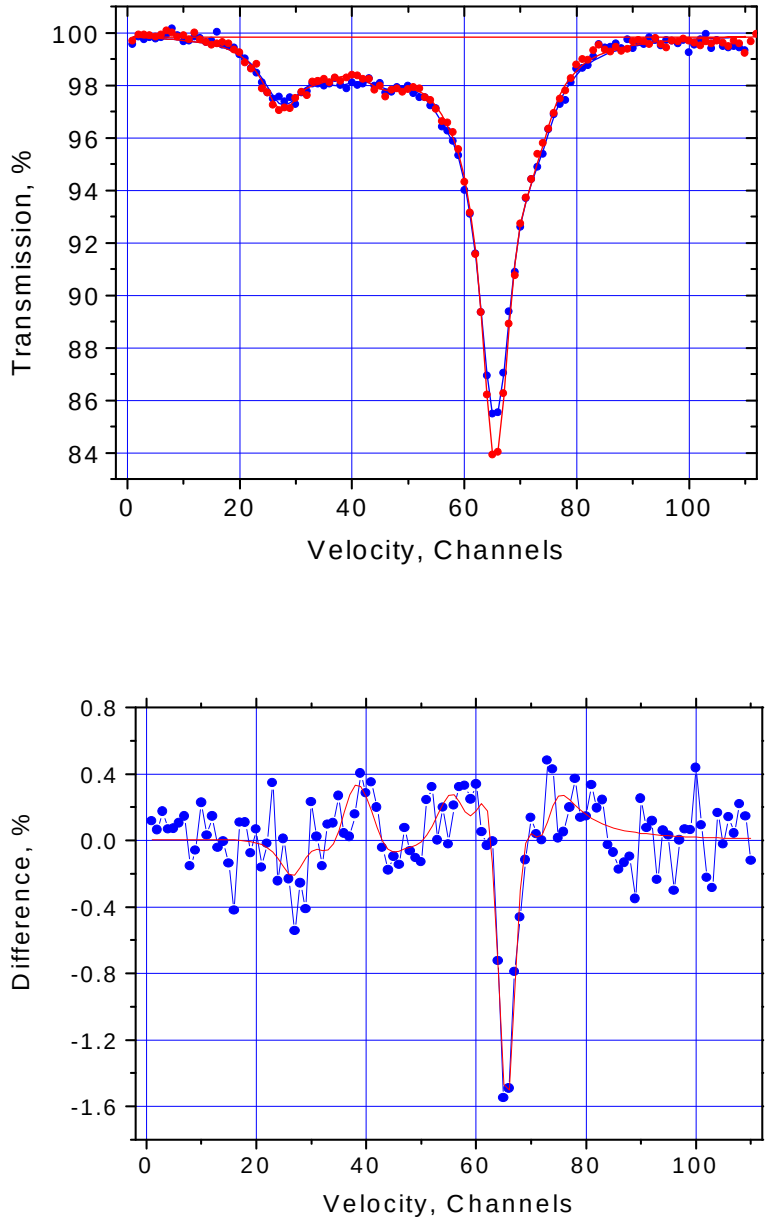

Fig. 24. Mössbauer spectrum and "with/without laser" difference for the third sample of $^{57}Fe^{2+} : MgO$.

transformation of the Mössbauer spectrum. The first explanation which comes to mind is the excitation of sound inside the sample by pulsed laser radiation. The possible mechanism of this excitation is local heating of the sample and subsequent thermal expansion of the heated part. Consequently, the Mössbauer resonances are affected in the same way as was discussed previously in Chapter II, section A. Let us examine this possibility more carefully.

The observed modifications of the Mössbauer spectrum would require the frequency of the sound to be of the order of change in the Mössbauer linewidth, i.e. several megahertz. Furthermore, the long lifetime of the observed changes compared to the sound period implies high Q-factor of the sound inside the crystal. This means that the crystal should serve as a cavity for the sound wave. Taking into account sound velocity in MgO (9150 m/s for the longitudinal sound and 6620 m/s for the transverse sound) and crystal dimensions ($10 \times 10 \times 0.5\ mm^3$) we find that the crystal can accommodate sound of 4.5 MHz and higher frequencies for the longitudinal mode and 3.3 MHz and higher for the transverse mode. Excitation of ultrasound of these resonant frequencies could possibly explain broadening of the Mössbauer line. However, the appearance of new resonances cannot be explained by ultrasound for the following reasons. First of all, new lines appear far away from the initial one ($1 \div 2\ mm/s$). This would require $10 \div 20\ MHz$ ultrasound. It is very unlikely that such a high-frequency ultrasound could be excited by laser pulses whose power spectrum is much narrower. Secondly, if the observed Mössbauer changes were due to ultrasound effects, sound satellittes should have appeared symmetrically with respect to the original line. However, in Fig.21 we see that the additional lines are distributed non-symmetrically.

In order to test ultrasound explanation of the original line broadening, the following experiment was performed. Since one expects excitation of resonant sound,

it does not matter in which part of the sample it was initially excited. After a very short (compared to 40 μs) time sound vibration will be distributed uniformly all over the sample. Thus, the illumination of one part of the sample with a laser and simultaneous observation of Mössbauer modification in the other part would lead to the same difference in the "laser On/Off" spectra. In the experiment the illuminated area was shifted from the Mössbauer aperture so that they do not overlap. The result is that no difference in "laser On/Off" spectra was observed in this experiment. This fact provides rather convincing evidence that changes in nuclear absorption observed previously were not due to the sound effects.

As was previously mentioned, new Mössbauer lines can be explained by population of some excited electronic states of Fe^{2+}-ion whose lifetime is 40 μs. This explanation is very likely since the corresponding lifetime lies within the range of population decay times of $3d \leftrightarrow 3d$ transitions of transition-metal ions. If this is the case, the new lines in the Mössbauer absorption correspond to nuclear transitions in the excited electronic state or states (more than one metastable states can be populated by laser pumping). However, the nature of this state(s) is still unclear now. Furthermore, this does not explain broadening of the original line.

Another possible explanation can be given on the basis of the fact that $^{57}Fe^{2+}MgO$ is Jahn-Teller crystal and that its Mössbauer spectra are strongly affected by electronic Orbach relaxation.

Orbach relaxation processes occur via higher-lying electronic states [68]. The electronic structure of Fe^{2+} in octahedral crystal field is shown in Fig.25. It originates from ^5D term of a free Fe^{2+} ion in the following way [64]. ^5D has spin $S = 2$ according to Hund's rule. Thus, there are 25 electronic states in total. They correspond to different orientations of spin and angular momentum. If placed in an octahedral crystal field, ^5D splits into two crystal levels ^5E_g and $^5T_{2g}$ the latter being the lowest

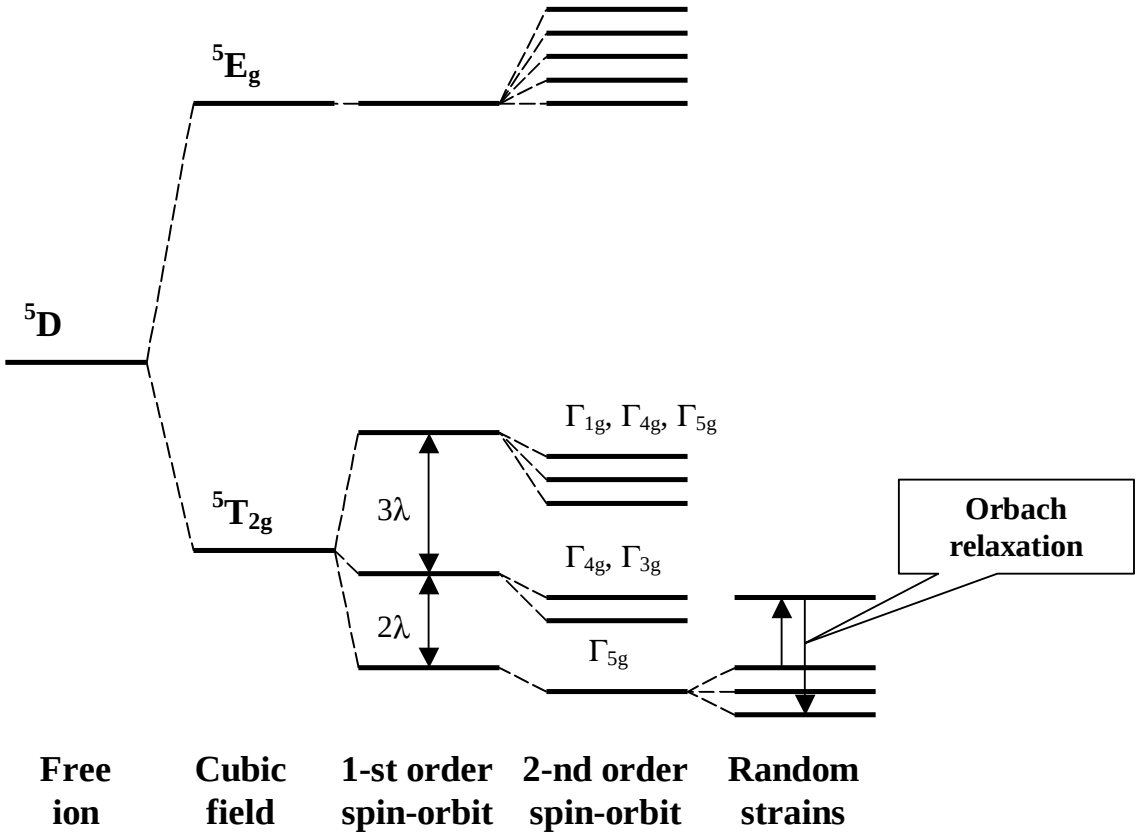

Fig. 25. Energy levels of Fe^{2+} in MgO [64].

one. Each of these levels is further split into a number of sublevels due to spin-orbit interaction. The first order spin-orbit coupling remains ${}^5E_g$ level unsplit while ${}^5T_{2g}$ splits into three states, Γ_{5g}, $\Gamma_{4g,3g}$, and $\Gamma_{1g,4g,5g}$ in the order of energy increase. Second order spin-orbit coupling lifts the degeneracy further: Γ_{5g} remains unsplit, $\Gamma_{4g,3g}$ and $\Gamma_{1g,4g,5g}$ split into 2 and 3 sublevels respectively, while ${}^5E_g$ state is split into five. The ground state of the system is Γ_{5g} triplet state. The magnitudes of the splittings discussed above are as follows: $\Delta E_{{}^5E \leftrightarrow {}^5T} = 10Dq \approx 10^4\ cm^{-1}$, $\Delta E_{\Gamma_{5g} \leftrightarrow \Gamma_{4g,3g}} = 2\lambda \approx 200\ cm^{-1}$, $\Delta E_{\Gamma_{4g,3g} \leftrightarrow \Gamma_{1g,4g,5g}} = 3\lambda \approx 300\ cm^{-1}$, and second order spin-orbit contribution is of the order $\sim 10\ cm^{-1}$. The ground-state triplet is split further by random strains inside the crystal. The magnitude of this splitting is $\sim 10^{-2}\ cm^{-1}$ [67].

In addition to octahedral crystal field, Jahn-Teller interaction occurs [69]. Its origin is related to the fact that octahedral symmetry of the site is not energetically favorable, i.e. if octahedral symmetry is slightly broken, the system energy goes down. There are several configurational states in which system energy is lower than in pure octahedral field. Moreover, the energy of all these configurations is the same, so that it is very easy to flip from one configuration to another. This is so called dynamic Jahn-Teller effect. There also exists another type of Jahn-Teller interaction when there is only one energetically preferable configuration with lower symmetry. This is called static Jahn-Teller effect. In some sense, the experiments with sodium nitroprusside described above (see Chapter II, section C) dealt with excitation of a very long-lived configurational state. This can be viewed as static Jahn-Teller effect.

Dynamic Jahn-Teller effect leads to significant changes in the energies of electronic states and the corresponding g-factors. In case of $Fe^{2+} : MgO$ Jahn-Teller interaction leads to significant decrease in energies of Γ_{4g} and Γ_{3g} levels (approximately, by a factor of 2). This makes Orbach relaxation between the ground-state

strain-split sublevels via intermediate $\Gamma_{4g,3g}$ states more efficient since Orbach relaxation rate is proportional to $\exp(-\Delta/kT)$.

Each of the three ground-state sublevels give rise to quadrupole splitting of nuclear sublevels. Since these states originate from the same triplet level, the magnitudes of all three quadrupole splittings are the same. However, Orbach relaxation efficiently reduces the quadrupole interaction amplitude. In work [70] it was shown that the shape of the Mössbauer line in case of relaxation effects can be described by the following formula:

$$P(\omega) = \frac{2}{\Gamma}\frac{\omega^2(3W+\Gamma) + \left(3W+\frac{\Gamma}{2}\right)\left(Q^2-\omega^2+\frac{3}{2}W\Gamma+\frac{1}{4}\Gamma^2\right)}{\omega^2(3W+\Gamma)^2 + \left(Q^2-\omega^2+\frac{3}{2}W\Gamma+\frac{1}{4}\Gamma^2\right)^2}. \tag{4.4}$$

Here Γ is the natural nuclear linewidth, W is the rate of flips between the three states of the ground-state triplet, Q is the quadrupole splitting, and ω is the frequency of the incident γ-radiation. It is easy to see that this shape approaches single line as $W \to \infty$ and it approaches quadrupole doublet as $W \to 0$.

Taking into account the above information about Jahn-Teller effect and Orbach relaxation, it is rather reasonable to assume that laser excites some hypothetical metastable configurational state and shifts $\Gamma_{4g,3g}$ levels to higher energies. Consequently, Orbach relaxation rate reduces and the Mössbauer line becomes broader. This is consistent with the behavior of unperturbed Mössbauer spectra at different temperatures in such a sense that spectra become broader at lower temperatures and, correspondingly, at lower relaxation rates W. Observation of metastable long-lived optically-excited configurational states in sodium nitroprusside supports the possibility of existence of such a state in iron-doped magnesium oxide. Thus, excitation of metastable configurational state together with optical population of metastable electronic state(s) could explain the observed transformations of the Mössbauer spec-

tra. However, to clarify the origin of the observed changes, further investigation is required. It can include possible studies of the sample by X-ray or neutron diffraction under laser excitation, far-infrared spectroscopy, etc.

CHAPTER V

CONCLUSION

In the present work a possibility of manipulating Mössbauer absorption spectra have been analyzed both theoretically and experimentally. The theoretical results can be summarized as follows:

- A theoretical model describing a possibility of optical modification of nuclear resonant spectra via electronic degrees of freedom is developed. It is shown that in the simplest situation one comes to a four-level model for the combined electron-nuclear system in the case of isomer shift of atomic levels, but it might be more complicated if hyperfine splittings are present in the system. The model describes how electronic excitation caused by optical field can be transferred to the nucleus via hyperfine interaction.

- Different types of hyperfine interactions are analyzed in view of optical driving of nuclear transitions. In the case of isomer shift of atomic levels, the predicted effects are the appearance of a new line in the Mössbauer absorption, power broadening of nuclear transitions caused by laser radiation, their Rabi splitting, and vanishing of hyperfine interaction if the optical driving becomes strong. Two additional effects could be observed if the ground state of the medium is hyperfine split. These are optical pumping of nuclear hyperfine sublevels and coherent population trapping effects. In the former case, optical pumping would lead to redistribution of absorption strength among Mössbauer lines while in the latter case complete cancellation of nuclear absorption can be expected.

As for the experimental part of the work, the following results have been obtained:

- Suitable Mössbauer-active media for the first proof-of-principle experiment have been found. Among them are some optical crystals doped with divalent or trivalent iron and crystals doped with rare-earths, primarily europium and samarium.

- Various crystal samples containing ^{57}Fe and ^{151}Eu were prepared and analyzed by means of optical and Mössbauer spectroscopic techniques. $^{57}Fe^{2+} : MgO$ appeared to be the most suitable for laser-Mössbauer experiment.

- Mössbauer and optical spectra were obtained for the sample of $^{57}Fe^{2+} : MgO$ under study. Thermal behavior of Mössbauer absorption of the sample suggested importance of relaxation processes.

- Laser Mössbauer experiment was performed. The spectra modified by laser action were analyzed and laser effect on the Mössbauer absorption was established. Under laser action the existing Mössbauer resonances drop in amplitude and become broader and new absorption lines appear.

- The observed changes in the Mössbauer spectra can be attributed to excitation of metastable electronic or configurational states. However, further investigation is needed to clarify the origin of the observed effects.

REFERENCES

[1] O. Kocharovskaya, R.D. Li, and P. Mandel, Opt. Commun., **77**, 215 (1990); O. Kocharovskaya, P. Mandel, and Y.V. Radeonychev, Phys. Rev. A, **45**, 1997 (1992); O. Kocharovskaya, Phys. Rep., **219**, 175 (1992); J. Mompart and R. Corbalan, J. Opt. B, **2**, R7 (2000).

[2] S.E. Harris, Phys. Today, **50**, 36 (1997); J.P. Marangos, J. Mod. Opt., **45**, 471 (1998).

[3] M.D. Lukin, S.F. Yelin, A.S. Zibrov, and M.O. Scully, Laser Physics, **9**, 759 (1999).

[4] A.S. Zibrov, M.D. Lukin, D.E. Nikonov, et al., Laser Physics, **5**, 553 (1995).

[5] A.S. Zibrov, M.D. Lukin, L. Hollberg, et al., Phys. Rev. Lett., **76**, 3935 (1996).

[6] A.S. Zibrov, M.D. Lukin, D.E. Nikonov, et al., Phys. Rev. Lett., **75**, 1499 (1995).

[7] M. Bajcsy, A.S. Zibrov, and M.D. Lukin, Nature, **426**, 638 (2003).

[8] M.O. Scully and M.S. Zubairy, Science, **301**, 181 (2003).

[9] S. E. Harris and A. V. Sokolov, Phys. Rev. Lett., **81**, 2894 (1998); S. E. Harris and A. V. Sokolov, Phys. Rev. A, **55**, R4019 (1997); F. L. Kien, J. Q. Liang, and M. Katsuragawa et al., Phys. Rev. A, **60**, 1562 (1999); A. V. Sokolov, D. R. Walker, D. D. Yavuz, G. Y. Yin, and S. E. Harris, Phys. Rev. Lett., **85**, 562 (2000); K. Hakuta, M. Suzuki, M. Katsuragawa, and J. Z. Li, Phys. Rev. Lett., **79**, 209 (1997).

[10] R. Kolesov, Phys. Rev. A, **64**, art. no. 063819 (2001); R. Kolesov and O. Kocharovskaya, Phys. Rev. A, **67**, art. no. 023810 (2003).

[11] P.M. Anisimov, R.A. Akhmedzhanov, I.V. Zelenskii, R.L. Kolesov, and E.A. Kuznetsova, JETP, **96**, 801 (2003); R. Akhmedzhanov, I. Zelensky, R. Kolesov, and E. Kuznetsova, Phys. Rev. E, **69**, art. no. 036409 (2004).

[12] I. Novikova and G.R. Welch, J. Mod. Opt., **49**, 349 (2002).

[13] R.L. Mössbauer, Z. Phys., **151**, 124 (1958); R.L. Mössbauer, Naturwissenshaften, **45**, 538 (1958); R.L. Mössbauer, Z. Naturforsch., **14a**, 211 (1959).

[14] N.N. Greenwood and T.C. Gibb, *Mossbauer Spectroscopy* (Chapman and Hill, London, 1971); T.E. Granshaw et al., *Mössbauer Spectroscopy and its Applications* (Cambridge University Press, New York, 1985).

[15] O. Kocharovskaya, R. Kolesov, and Y. Rostovtsev, Phys. Rev. Lett., **82**, 3593 (1999); Y. Rostovtsev, R. Kolesov, and O. Kocharovskaya, Hyperfine Interactions, **143**, 121 (2002).

[16] O. Kocharovskaya, R. Kolesov, and Y. Rostovtsev, Laser Physics, **9**, 745 (1999); R. Kolesov, Y. Rostovtsev, O. Kocharovskaya, Opt. Commun., **179**, 537 (2000).

[17] N.D. Heiman, L. Pfeiffer, and J.C. Walker, Phys. Rev. Lett., **21**, 93 (1968).

[18] G.J. Perlow, Phys. Rev., **172**, 319 (1968).

[19] E. Ikonen, P. Helisto, T. Katila, and K. Riski, Phys. Rev. A, **32**, 2298 (1985); E. Ikonen, P. Helisto, J. Hietaniemi, and T. Katila, Phys. Rev. Lett., **60**, 643 (1988); E. Ikonen, J. Hietaniemi, and T. Katila, Phys. Rev. B, **38**, 6380 (1988).

[20] E. Kuznetsova, R. Kolesov, and O. Kocharovskaya, Phys. Rev. A, **68**, art. no. 043825 (2003).

[21] P. Helisto, I. Tittonen, M. Lippmaa, and T. Katila, Phys. Rev. Lett., **66**, 2037 (1991).

[22] F.J. Lynch, R.E. Holland, and M. Hamermesh, Phys. Rev., **120**, 513 (1960).

[23] G.V. Smirnov, U. vanBurck, J. Arthur, et al., Phys. Rev. Lett., **77**, 183 (1996).

[24] F.G. Vagizov, Hyperfine Interact., **61**, 1359 (1990).

[25] U. Hauser, V. Oestreich, and H.D. Rohrweck, Z. Phys. A, **280**, 17 (1977); U. Hauser, V. Oestreich, and H.D. Rohrweck, Z. Phys. A, **284**, 9 (1978).

[26] J.A. Guida, O.E. Piro, and P.J. Aymonino, Sol. State Commun., **66**, 1007 (1988).

[27] M. Rüdlinger, J. Schefer, T. Vogt, et al., Physica B, **180& 181**, 293 (1992); Th. Woike, H. Zöllner, W. Krasser, and S. Haussühl, Sol. State Commun., **73**, 149 (1990).

[28] G. Shimkaveg, W.W. Quivers Jr., R.R. Dasari, et al., Phys. Rev. Lett., **53**, 2230 (1984).

[29] S.G. Bishop, in *Deep Centers in Semiconductors* (Ed. S. Pantelides), p. 667 (Gordon and Breach, New York, 1985).

[30] B.S. Ham and P.R. Hemmer, Phys. Rev. Lett., **84**, 4080 (2000).

[31] C.D. Jeffries, Phys. Rev. Lett., **19**, 1221 (1967); L.F. Mollenauer, W.B. Grant, and C.D. Jeffries, Phys. Rev. Lett., **20**, 488 (1968); W.B. Grant, L.F. Mollenauer, and C.D. Jeffries, Phys. Rev. B, **4**, 1428 (1971).

[32] F.D. Colegrove, L.D. Schearer, and G.K. Walters, Phys. Rev., **132**, 2561 (1963).

[33] R. Kolesov and E. Kuznetsova, Phys. Rev. B, **63**, art. no. 184107 (2001).

[34] E. Arimondo, Prog. Opt., **35**, 257 (1996).

[35] C.A. Morrison and R.P. Leavitt, in: *Handbook on the Physics and Chemistry of Rare Earths*, Vol. 5, edited by K.A. Gschneidner Jr. and L. Eyring (North-Holland, Amsterdam, 1982).

[36] *Handbook on the Physics and Chemistry of the Actinides*, edited by A.J. Freeman and G.H. Lander, North-Holland, Amsterdam (1984).

[37] C.J. Ballhausen, *Introduction to Ligand Field Theory* (McGraw-Hill, New York, 1962).

[38] T. Abritta, F. de Souza Barros, and N.T. Melamed, J. Lum., **33**, 141 (1985); T. Abritta and F. de Souza Barros, J. Lum., **40&41**, 187 (1988).

[39] J. Maria Neto, T. Abritta, F. de Souza Barros, and N.T. Melamed, J. Lum., **22**, 109 (1981).

[40] D.T. Palumbo, J. Lum., **4**, 89 (1971).

[41] L.P. Sosman, A. Dias Tavares, P.S. Silva, and T. Abritta, Phys. Stat. Sol. A, **176**, 1085 (1999).

[42] G. Walker and T.J. Glynn, J. Lum., **54**, 131 (1992).

[43] D. Walsh and J. Lange, Phys. Rev. B, **23**, 8 (1981); A. Poirier and D. Walsh, J. Phys. C: Sol. State, **16**, 2619 (1983).

[44] M. Nogami, T. Ishikawa, and T. Hayakawa, J. Lum., **96**, 163 (2002).

[45] J.P.D. Martin, M.J. Sellars, P. Tuthill, et al., J. Lum., **78**, 19 (1998).

[46] R.J. Hamers, J.R. Wietfeldt, and J.C. Wright, J. Chem. Phys., **77**, 683 (1982).

[47] J. Dexpert-Ghys, R. Mauricot, and M.D. Faucher, J. Lum., **69**, 203 (1996).

[48] R.M. Macfarlane, R.M. Shelby, A.Z. Genack, and D.A. Weitz, Opt. Lett., **5**, 462 (1980).

[49] K. Binnemans and C. Görller-Walrand, J. Alloys Compounds, **250**, 326 (1997); G. Blasse, G.J. Dirksen, and J.P.M Van Vliet, Inorg. Chim. Acta, **142**, 165 (1988).

[50] Electric quadrupole moment for the 21.5 keV state of ^{151}Eu as well as the probability of populating the excited state of Mössbauer transition of ^{149}Sm in ^{149}Eu decay are taken from Isotope Explorer Database http://ie.lbl.gov/endsf/.

[51] D.M. Boye, R.M. Macfarlane, Y. Sun, and R. S. Meltzer, Phys. Rev. B, **54**, 6263 (1996).

[52] Z. Hasan Z, L. Biyikli, J. Opt. Soc. Am. B, **18**, 232 (2001); L. Biyikli, Z. Hasan Z, J. Lum., **83-84**, 373 (1999); N. Yamashita, O. Harada, and K. Nakamura, Jap. J. Appl. Phys., Part 1, **34** 5539 (1995).

[53] H.J. Seo, B.K. Moon, T. Tsuboi, J. Lum., **87-89**, 1059 (2000).

[54] M. Eibschütz, R.L. Cohen, E. Buehler, and J.H. Wernick, Phys. Rev. B, **6**, 18 (1972).

[55] J.-P.R. Wells and R.J. Reeves, Phys. Rev. B, **61**, 13593 (2000).

[56] J.F. Martela, S. Jandla, B. Vianab, and D. Vivienb, J. Phys. Chem. Solids, **61**, 1455 (2000).

[57] S. Kück, Appl. Phys. B, **72**, 515 (2001).

[58] O. Leupold, A.I. Chumakov, E.E. Alp, et al., Hyperfine Intaractions, **123**, 611 (1999).

[59] Z.J. Kiss, Phys. Rev., **127**, 718 (1962).

[60] R.C. Duncan Jr. and Z.J. Kiss, Appl. Phys. Lett., **3**, 23 (1963).

[61] G.V. Smirnov, Hyperfine Interactions, **125**, 91 (2000); G.V. Smirnov, Hyperfine Interactions, **123**, 31 (1999).

[62] Prof. E.E. Alp, Advanced Photon Source Facility at Argonne National Laboratory, private communication.

[63] F. Vagizov, R. Kolesov, and O. Kocharovskaya, J. Mod. Opt., submitted.

[64] W. Low and M. Weger, Phys. Rev., **118** 1119 (1960); W. Low and M. Weger, Phys. Rev., **118** 1130 (1960).

[65] N.B. Manson, J.T. Gourley, E.R. Vance, et al., J. Phys. Chem. Solids, **37**, 1145 (1976); F.A. Modine, E. Sonder, and R.A. Weeks, J. Appl. Phys., **48**, 3514 (1977).

[66] D.N. Pipkorn and H.R. Leider, Bull. Am. Phys. Soc., bf 11, 49 (1966).

[67] F.S. Ham, Phys.Rev., **160**, 328 (1967).

[68] R. Orbach, Proc. Roy. Soc. (London), **A264**, 458 (1961).

[69] A. Hjortsberg, J.T. Vallin, and F.S. Ham, Phys. Rev. B, **37**, 3196 (1988).

[70] J.A. Tjon and M. Blume, Phys. Rev., **165**, 456 (1968).

VITA

Roman L. Kolesov - Curriculum Vita

Personal Information

Born: 1977, Nizhny Novgorod, Russia.

Address: 9-a Strokin Str. Apt.9, Nizhny Novgorod, 603138, Russia.

Education:

2004 : Doctorate of Philosophy, Physics; Texas A&M University.

1998: Master of Science, Physics; Nizhny Novgorod State University, Russia.

1996: Bachelor of Science, Physics; Nizhny Novgorod State University, Russia.

Honors/Awards

1994 - Soros Scholarship.

1994 - Sakharov Scholarship.

1995-1998 - Scholarship of the President of Russian Federation.

2000 - The best student at the *XXX International Conference on Mössbauer Effect: Materials, Magnetism, and Gamma-Optics*, Kazan, Russia.

2000 - The best student work at the *Texas Section APS Meeting*, College Station, Texas A&M University.

2001 - Award for Outstanding Graduate Performance in Pre-Dissertation Physics Research/Academics at Texas A&M University.

Publications:

1. O. Kocharovskaya, R. Kolesov, and Y. Rostovtsev, Phys. Rev. Lett., **82**, 3593 (1999).
2. O. Kocharovskaya, R. Kolesov, and Y. Rostovtsev, Laser Physics, **9**, 745 (1999).
3. R. Kolesov, Y. Rostovtsev, and O. Kocharovskaya, Opt. Commun., **179**, 537 (2000).
4. R. Kolesov, Phys. Rev. A, **64**, art. no. 063819 (2001).
5. R. Kolesov and E. Kuznetsova, Phys. Rev. B, **63**, art. no. 184107 (2001).
6. Y. Rostovtsev, R. Kolesov, and O. Kocharovskaya, Hyperfine Interactions, **143**, 121 (2002).
7. E. Kuznetsova, R. Kolesov, and O. Kocharovskaya, Phys. Rev. A, **68**, art. no. 043825 (2003).
8. P.M. Anisimov, R.A. Akhmedzhanov, I.V. Zelenskii, R.L. Kolesov, and E.A. Kuznetsova, JETP, **96**, 801 (2003).
9. R. Kolesov and O. Kocharovskaya, Phys. Rev. A, **67**, art. no. 023810 (2003).
10. R. Akhmedzhanov, I. Zelensky, R. Kolesov, and E. Kuznetsova, Phys. Rev. E, , **69**, art. no. 036409 (2004).

The typist for this thesis was Roman L. Kolesov.